Repeated Random Sampling for Minimizing the Time-to-Accuracy of Learning

Patrik Okanovic [*1] **Roger Waleffe** [*2] **Vasilis Mageirakos** [1] **Konstantinos E. Nikolakakis** [3] **Amin Karbasi** [3 4]
Dionysis Kalogerias [3] **Nezihe Merve Gürel** [5] **Theodoros Rekatsinas** [1]

Abstract

Methods for carefully selecting or generating a small set of training data to learn from, i.e., data pruning, coreset selection, and data distillation, have been shown to be effective in reducing the ever-increasing cost of training neural networks. Behind this success are rigorously designed strategies for identifying informative training examples out of large datasets. However, these strategies come with additional computational costs associated with subset selection or data distillation before training begins, and furthermore, many are shown to under-perform random sampling in high data compression regimes. As such, many existing methods may not reduce 'time-to-accuracy', which has become a critical efficiency measure of training deep neural networks over large datasets. In this work, we revisit a powerful yet overlooked random sampling strategy to address these challenges and introduce an approach called *Repeated Sampling of Random Subsets* (RSRS or RS2), where we randomly sample the subset of training data for each epoch of model training. We test RS2 against thirty state-of-the-art data pruning and data distillation methods across four datasets including ImageNet. Our results demonstrate that RS2 significantly reduces time-to-accuracy compared to existing techniques. For example, when training on ImageNet, RS2 yields accuracy improvements up to 29% compared to competing pruning methods while offering a runtime reduction of 7×. Beyond the above meta-study, we provide a convergence analysis for RS2 and discuss its generalization capability. The primary goal of our work is to establish RS2 as a competitive baseline for future data selection or distillation techniques aimed at efficient training.

[*]Equal contribution [1]ETH Zürich [2]University of Wisconsin-Madison [3]Yale [4]Google Research [5]Tu Delft. Correspondence to: Roger Waleffe <waleffe@wisc.edu>.

Data-centric Machine Learning Research (DMLR) Workshop at the 40^{th} International Conference on Machine Learning, Honolulu, Hawaii, USA. 2023.

1. Introduction

Deep learning is continually achieving impressive results, from image classification (He et al., 2016; Dosovitskiy et al., 2020) to speech recognition (Chiu et al., 2018) and natural language processing (Brown et al., 2020; Radford et al., 2019; OpenAI, 2023). Much of this success can be attributed to training large neural networks over datasets with millions or billions of examples (Russakovsky et al., 2015; Gokaslan & Cohen, 2019; Brown et al., 2020; Radford et al., 2021). However, these network and dataset sizes lead to model training that requires weeks or months and yields significant monetary and computational costs (Mindermann et al., 2022; Brown et al., 2020). Such costs nearly prohibit further model refinement through hyperparameter search or neural architecture search. As a result, there has been an arms race to minimize the required training time to reach a given accuracy, i.e., time-to-accuracy.

To reduce time-to-accuracy, recent works focus on decreasing the amount of training data used for model learning during each epoch. More specifically, given a large, labeled dataset, these works aim to maximize end-model accuracy and minimize runtime when training for multiple rounds, where training within each round is performed only on a small set of examples equal in size to a fraction r of the full dataset. The set of examples used for training at each round can be either chosen once before learning begins or periodically recomputed between rounds based on model updates (e.g., as in Mirzasoleiman et al. (2020); Killamsetty et al. (2021b)). Existing methods in this framework span two main categories: 1) *data pruning* methods which aim to reduce time-to-accuracy by selecting a subset of the most informative examples for training (Welling, 2009; Bachem et al., 2015; Bateni et al., 2014; Chen et al., 2010; Killamsetty et al., 2021b; Paul et al., 2021; Mirzasoleiman et al., 2020; Sorscher et al., 2022); 2) *dataset distillation* methods which aim to achieve the same by generating small sets of synthetic examples that summarize training instances from the full dataset (Wang et al., 2018; Yu et al., 2023). We review data pruning and distillation methods in Section 2. Briefly, these methods have demonstrated strong competitiveness in minimizing the time-to-accuracy of learning and influenced a large number of subsequent works, including ours. However, several challenges persist in the pursuit of

minimizing time-to-accuracy using these methods. One major challenge lies in the time efficiency aspect, as there is a notable overhead associated with subset selection. For example, many methods require pretraining an auxiliary model on the full dataset for a few epochs in order to select the subset, a task which we find can take roughly 250 minutes on ImageNet (Figure 3b) while training itself with $r = 1$ and 10% takes only 40 and 400 minutes respectively. Even when efforts are made to address this issue, score-based data pruning has fallen short in achieving high accuracy, particularly in the high compression regime (small r) (Ayed & Hayou, 2023), a practical regime enabling ML practitioners to efficiently perform tasks such as hyperparameter selection and architecture search.

With these challenges in mind, in this work, we revisit the random sampling baseline for subset selection and introduce an intuitive and powerful extension of this method for optimizing the time-to-accuracy of learning. Random sampling is widely accepted as a competitive baseline, particularly for high compression regimes (Ayed & Hayou, 2023; Sorscher et al., 2022), whose success lies in the ability to select representative data examples for training, thus preventing overfitting. Typically, a static subset of the complete dataset is sampled once before the learning begins (Guo et al., 2022; Park et al., 2022). However, we believe that a better way to utilize this baseline is by repeatedly sampling data instances at each epoch, as this allows the learner to explore more previously unseen examples throughout training. Random exploration has already proven advantageous for data pruning methods, particularly in the high compression regime (Ayed & Hayou, 2023), allowing them to calibrate for distribution shift (caused by discarded examples). Moreover, adversarial training has also experienced time-to-accuracy reduction with random exploration (Kaufmann et al., 2022). Surprisingly, however, this method has yet to be studied or evaluated for standard training of deep neural networks. Motivated by this gap, we introduce Repeated Sampling of Random Subsets (RSRS = RS2), where we sample a subset uniformly at random for each training epoch. The main contribution of this paper is an in-depth analysis of RS2. We demonstrate that RS2 surpasses state-of-the-art data pruning and distillation methods in accuracy and runtime across a wide range of subset sizes. In addition, we show that it outperforms all prior methods in the high compression regime, thus, posing a strong benchmark to beat for minimizing time-to-accuracy. In Section 3, we provide a detailed explanation of RS2, and in Section 4 we discuss its convergence rate and generalization error.

We extensively evaluate the time-to-accuracy of RS2 and compare it against twenty-two proposed data pruning and eight data distillation methods from the literature (Section 5). We find that RS2 outperforms existing methods with respect to runtime and accuracy across varying subset selection sizes and datasets, including CIFAR10, CIFAR100, ImageNet30, and ImageNet itself. For example, when training a ResNet-18 in the high-compression regime (with $r = 10\%$) on ImageNet, RS2 yields a model with 66% accuracy, 11 points higher than the next-best method and only 3.5 points less than training with the entire dataset every round. Yet, RS2 reaches this accuracy $9\times$ faster than standard full-dataset training. With $r = 1\%$, RS2 still reaches 47% accuracy, while the next-best method achieves only 18%. Finally, we present an extension beyond supervised learning by evaluating RS2 for self-supervised pretraining of GPT2 (Radford et al., 2019), a setting for which existing works have yet to study. We find that RS2 can reduce training time by 3-10$\times$ while yielding models within 2 and 5 points of the full-dataset accuracy and perplexity respectively.

2. Preliminaries

We first present a unified framework for the problem of reducing time-to-accuracy by training on less data each epoch and review existing data pruning and distillation methods.

Problem Statement Given a large, labeled dataset $S = \{\mathbf{x}_i, y_i\}_{i=1}^N$, where each training example consists of an input feature vector $\mathbf{x}_i$ and a given ground truth label y_i, our goal is to minimize runtime and maximize accuracy when training for X rounds, with the training of each round performed on a set of examples S' with size $|S'| = r \cdot |S|$ for $r \in (0, 1]$.

We highlight two important points: First, it is generally assumed that X is chosen such that training proceeds for the same number of rounds as when training on the full dataset, otherwise the computational benefits are reduced (e.g., $r = 50\%$ with $X = 200$ is the same amount of computation as $r = 100\%$ with $X = 100$). Second, note that the subset S' may be static or vary across rounds. In fact, some existing methods periodically recompute S' between rounds (Mirzasoleiman et al., 2020; Killamsetty et al., 2021b), while others do not (Sorscher et al., 2022). Given the primary goal of minimizing time-to-accuracy, either choice is valid so long as the time to generate the subset S' at each round is included in the overall runtime.

Related Work To minimize time-to-accuracy, *data pruning* methods attempt to find a subset (also called a *coreset*) of informative examples $S' \subset S$ such that a model trained on S' achieves similar accuracy to a model trained on S (Guo et al., 2022; Park et al., 2022). Numerous metrics have been proposed to quantify importance: Uncertainty based methods such as Least Confidence, Entropy, and Margin (Sachdeva et al., 2021) assume examples with lower confidence will have higher impact on training. Loss and error based methods operate on a similar principle. Forgetting Events (Toneva et al., 2018), GraNd, EL2N (Paul et al.,

2021), and others (Bachem et al., 2015; Munteanu et al., 2018; Dasgupta et al., 2019; Liu et al., 2021) are examples of these methods. Other techniques for subset selection, such as CRAIG (Mirzasoleiman et al., 2020) and GradMatch (Killamsetty et al., 2021a), focus on gradient matching, where the goal is to construct a subset of examples such that a weighted sum of the model gradients on the subset matches the overall gradient on the full dataset. A different class of methods focuses on feature geometry for data subset selection. A number of geometry-based methods have been proposed, such as Herding (Welling, 2009; Chen et al., 2010), K-Center Greedy (Sener & Savarese, 2018), and prototypes (Sorscher et al., 2022). Additional data pruning algorithms attempt to find the training examples closest to the decision boundary (e.g., Adversarial Deepfool (Ducoffe & Precioso, 2018) and Contrastive Active Learning (Liu et al., 2021)), pose subset selection as a bilevel optimization problem (e.g., Retrieve (Killamsetty et al., 2021c) and Glister (Killamsetty et al., 2021b)), or connect subset selection to maximization of a submodular function (e.g., GraphCut, Facility Location, and Log Determinant (Iyer et al., 2021)). Active learning methods (which aim to minimize labeling cost by selecting an informative subset given a large unlabeled dataset), can also be used in the presence of a labeled dataset when the goal is to reduce time-to-accuracy. In fact, active learning has been shown to outperform existing methods in this setting (Park et al., 2022). We refer the reader to recent surveys (Guo et al., 2022) for more details on the above methods and for comparisons between them.

In contrast to data pruning which assumes S' to be a subset of S, *dataset distillation* methods use S to generate a small set of synthetic examples S' that aims to summarize S. Dataset distillation methods can be split into three groups: 1) Performance matching methods (Wang et al., 2018; Deng & Russakovsky, 2022) aim to optimize the synthetic examples in S' such that models trained on S' achieve the lowest loss on the original data S. 2) Parameter matching techniques (Zhao et al., 2021; Lee et al., 2022; Kim et al., 2022; Cazenavette et al., 2022) focus instead on matching the parameters of a network trained on S' with those of a network trained on S by training both models for a number of steps. 3) Finally, the distribution matching approach (Zhao & Bilen, 2023) to dataset distillation attempts to obtain synthetic examples in S' such that the distribution of S' matches the distribution of S. We refer the reader to (Yu et al., 2023) for a detailed survey on dataset distillation.

3. RS2: Repeated Random Sampling for Minimizing Time-to-Accuracy

We introduce the RS2 algorithm and discuss how it yields efficient training by reducing the amount of training data used at each round of model learning.

Repeated Sampling of Random Subsets (RS2) As discussed in Section 2, we assume access to a large, labeled dataset S and aim to minimize runtime while maximizing accuracy by training for X rounds. *We define RS2 as follows: Rather than traininng a model on the full dataset S for X rounds (i.e., epochs), train the same model for X rounds with the training of each round performed on a subset S' (of size $|S'| = r \cdot |S|$) sampled randomly from S (Algorithm 1).* Training within a round proceeds exactly the same when using S or S', except that S' has fewer examples (e.g., mini batches). We next describe RS2 in more detail and discuss two variants of the sampling strategy and the importance of appropriate learning rate scheduling.

Algorithm 1 RS2 General Algorithm

Require: Dataset $S = \{x_i, y_i\}_{i=1}^{N}$, selection ratio $r \in (0, 1]$, batch size b, initial model w^0, X rounds

$T \leftarrow \lceil N/b \rceil$
$t \leftarrow 1$
for round $j = 1$ to X **do**
  $S' \leftarrow randomly\_sample\_subset(S,\ r)$
  for $k = 1$ to $r \cdot T$ **do**
    batch $m \leftarrow S'[(k-1) \cdot b : k \cdot b]$
    $w^t \leftarrow train\_on\_batch(w^{t-1},\ m)$
    $t \leftarrow t + 1$
return w^t

RS2 With Replacement The simplest version of RS2 samples S' with replacement across rounds—sampling can be stratified. This means that examples included in the subset of previous rounds are replaced in S and eligible to be resampled when constructing S' for the current round, i.e., S' is always constructed by sampling uniformly from all examples in S.

RS2 Without Replacement A second variant of RS2 samples S' without replacement across rounds. That is, examples in S that have been included in the subset during previous rounds are not considered when sampling S' for the current round. This continues until all examples from S have been included in S' at some round, at which point all examples are once again eligible for subset selection and the process repeats. Observe that sampling S' without replacement across X rounds is equivalent to training on the full dataset S for $r \cdot X$ rounds (i.e., equivalent to *early stopping* after $r \cdot X$ rounds on the full dataset assuming the same randomn seed).

RS2 Hyperparameters For both RS2 variants, we assume that training proceeds using the same hyperparameters (e.g., batch size, optimizer, etc.) as those used when training on the full dataset with one exception: the learning rate schedule. The reason for this is that state-of-the-art training procedures often slowly decay the learning rate after each SGD step. We show in Figure 1 the common cosine annealing learning rate schedule (Loshchilov & Hut-

ter, 2016) used to train ResNets on CIFAR10. We include a vertical line showing the point of early stopping when running RS2 without replacement for $r = 10\%$. Observe that data pruning with RS2 (or any method) leads to fewer SGD iterations (even when training for the same X rounds). Thus, if the data pruning method uses the same learning rate schedule as when training on the full dataset, the learning rate may not decay to a sufficiently small value to achieve high end-model accuracy. We refer to this setting as *naive early stopping*. Instead, we train both RS2 variants with the same kind of learning rate schedule as when training the full dataset (e.g., cosine annealing), but we decay the learning rate faster with the decay rate inversely proportional to the subset size r (e.g., green line in Figure 1). This is standard across existing data pruning methods (Guo et al., 2022).

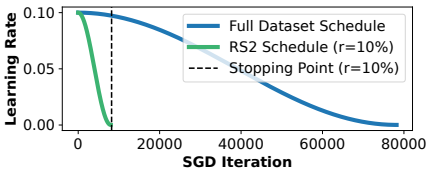

Figure 1: Learning rate schedules on CIFAR10 with and without data pruning.

Naive early stopping results in worse accuracy than RS2 with the modified learning rate schedule. For example, on CIFAR10 with $r = 10\%$, the former achieves 83.9% accuracy while RS2 with replacement reaches 89.7% and RS2 without replacement (i.e., early stopping with faster learning rate decay) reaches 91.7%. While we generally see RS2 without replacement outperform RS2 with replacement in terms of accuracy, we do not claim that one variant is strictly better in this paper. We refer the reader to existing works which study this problem (Haochen & Sra, 2019; Lu et al., 2022; De Sa, 2020).

4. Theoretical Analysis of RS2

With time-to-accuracy in mind, we now study the convergence rate and generalization error of RS2.

RS2 Convergence Rate We show that RS2 without replacement, under the assumptions described in Appendix E, converges at the same rate with respect to SGD iterations as standard training on the full dataset. For the convergence rate analysis, we assume $train\_on\_batch(w^{t-1},\ m)$ in Algorithm 1 uses Nesterov's accelerated gradient descent (Nesterov, 1983) as shown in Algorithm 2. Following the analysis of recent works on the performance of accelerated mini-batch SGD (Ghadimi & Lan, 2016), we have:

Corollary 4.1. *Suppose the loss $l(w)$ is nonconvex, has β-Lipschitz continuous gradients, and is bounded below. Let $g(w, \xi_t)$ at step t represent the gradient estimate used when updating the model as in Algorithm 2 in the Appendix. Assume the gradient estimate satisfies $\mathbb{E}\left[||g(w,\xi_t) - \nabla l(w)||^2\right] \leq \sigma^2$, and $\mathbb{E}[g(w,\xi_t)] = \nabla l(w)$, where ξ_t are random vectors whose distributions are supported on $\Xi_t \in \mathbb{R}^d$. With the previous assumptions, using a selection ratio $r \in (0, 1]$ and mini batch of size b, RS2 produces an iterate w after X rounds, with rT batches per round, such that:*

$$\mathbb{E}\left[||\nabla l(w)||^2\right] \leq \mathcal{O}\left(\frac{\beta(l(w^0) - l(w^*))}{r \cdot T \cdot X} + \frac{\sigma\sqrt{\beta(l(w^0) - l(w^*))}}{\sqrt{b \cdot r \cdot T \cdot X}}\right). \tag{1}$$

We discuss the assumptions and prove Corollary 4.1 in Appendix E. We find that the convergence rate of RS2 compared to the full dataset convergence rate (Ghadimi & Lan, 2016) has a scaling factor r in front of the total number of iterates, while the bound remains consistent with respect to all the other parameters; With $r = 1$ we recover the results from previous work (Ghadimi & Lan, 2016). When $r < 1$ the gradient bound after X rounds increases compared to training with the full dataset for X rounds, but this is intuitive as each round contains fewer mini batches (rT with $r < 1$ instead of T). If RS2 with $r < 1$ is instead allowed to train for more rounds, specifically $X_{new} = \frac{X}{r}$, then both training RS2 for X_{new} rounds and training on the full dataset for X rounds result in the same number of mini-batch iterations (TX). In this case, the gradient is bounded by the same value, implying that RS2 and training on the full dataset converge with respect to *mini-batch iterations* at the same rate. Overall, Corollary 4.1 ties the convergence behavior of RS2 directly to the amount of pruning r and to training on the full dataset.

RS2 Generalization Error We now provide an upper bound on the generalization error of RS2. Here, we relax the update rule from Algorithm 1 to a standard gradient update without momentum. Recall that as r decreases, RS2 results in a smaller total number of gradient steps after X rounds compared to $r = 1$. While this may lead to an increase in optimization error, the generalization error is expected to be smaller than that of the full dataset schedule (shorter training time gives a smaller generalization error). This phenomenon has been characterized rigorously in prior works (Hardt et al., 2016) for vanilla SGD with batch size $b = 1$, however it does not directly apply to larger mini batch sizes and general selection rules. As such, we show an extension of known generalization error bounds that also holds for RS2 with mini batch size b. Before we proceed, we first introduce some notation for brevity. We define the training dataset $S \triangleq (z_1, z_2, \ldots, z_N)$, for which $z_i \triangleq (\mathbf{x}_i, y_i)$ for $i \in \{1, \ldots, n\}$ and the (empirical) loss $l(w) \triangleq \frac{1}{N}\sum_{i=1}^{N} f(w, z_i)$, where $f : \mathbb{R}^d \times \mathcal{Z} \to \mathbb{R}^+$. Let $z_1, z_2, \ldots, z_N, z$ be i.i.d random variables with respect to an unknown distribution $\mathcal{D}$. Then for any stochastic algorithm A with input S, and output $A(S)$, the generalization error ϵ_{gen} is defined as the difference between the empirical and

population loss (Hardt et al., 2016):

$$\epsilon_{\text{gen}}(f, \mathcal{D}, A) \triangleq \mathbb{E}_{S,A,z}\big[f(A(S), z)\big] - \mathbb{E}_{S,A}\Big[\frac{1}{N}\sum_{i=1}^{N} f(A(S), z_i)\Big]. \tag{2}$$

We now proceed with an upper bound on the generalization error of RS2. The next result follows from recent work (Nikolakakis et al., 2023), and applies to RS2 with no momentum and any batch size b.

Theorem 4.2 (Generalization error RS2, (Nikolakakis et al., 2023) Theorem 8)**.** *Let the function f be nonconvex, L_f-Lipschitz and β_f-smooth. Then the generalization error of the standard gradient RS2 algorithm with a decreasing step-size $\eta_t \leq C/t$ (for $C < 1/\beta_f$), is bounded as:*

$$|\epsilon_{\text{gen}}(f, \mathcal{D}, \text{RS2})| \leq \frac{1}{N} \cdot 2Ce^{C\beta_f} L_f^2 (r \cdot T \cdot X)^{C\beta_f} \cdot \min\Big\{1 + \frac{1}{C\beta_f}, \log(e \cdot r \cdot T \cdot X)\Big\}. \tag{3}$$

The proof of Theorem 4.2 follows from recent work (Nikolakakis et al., 2023) (Appendix F). Observe that, as above for the convergence rate, when comparing the generalization error of RS2 to that of the full dataset (Nikolakakis et al., 2023), the dependence on all parameters remains the same except that the number of iterates for RS2 is scaled by r. The generalization error of RS2 relies on the fact that the batch at each iteration is selected *non-adaptively and in a data-independent fashion*. However, most data pruning methods adopt data-dependent strategies, and deriving the relationship between the generalization error of RS2 and that of any arbitrary data-dependent method can be challenging. A recent finding on the generalization of data-dependent pruning, particularly for small r, shows data-dependency may worsen the generalization (Ayed & Hayou, 2023) due to the distribution shift caused by discarding a large number of data examples during training, thus leading to inferior performance compared to random sampling.

5. Evaluation

We evaluate RS2 on four common benchmarks for supervised learning and compare against existing data pruning and distillation methods. We show that:

1. Across a wide range of pruning ratios, RS2 reaches higher accuracy than all existing methods.
2. For a given pruning ratio, RS2 also trains the fastest, and thus has the fastest time-to-accuracy.
3. In the presence of noisy labels, RS2 is the most robust data pruning method; It achieves the highest end-model accuracy and lowest relative drop in performance vs. training on the clean dataset.

We also show that RS2 can extend beyond conventional supervised learning and reduce the self-supervised pretraining cost of GPT models with little model quality loss.

5.1. Experimental Setup

We first discuss the setup used in the experiments. More details can be found in Appendix B.

Datasets, Models, and Metrics We benchmark RS2 against baseline methods using CIFAR10 (Krizhevsky et al., 2009), CIFAR100 (Krizhevsky et al., 2009), ImageNet30 (Hendrycks et al., 2019), and ImageNet (Russakovsky et al., 2015). We train ResNet models (He et al., 2016) representative of modern state-of-the-art convolutional neural networks. Beyond the standard supervised setting, we also evaluate RS2 when training GPT2 (Radford et al., 2019) on the OpenWebText dataset (Gokaslan & Cohen, 2019). In this setting, we measure zero-shot final word accuracy on the LAMBADA dataset (Paperno et al., 2016) and perplexity on LAMBADA and WikiText103 (Merity et al., 2016). For all experiments we measure subset selection overhead, overall training time (including the total time for subset selection across all rounds and the total training time on selected subsets), and end-model accuracy.

Baselines We compare RS2 against 22 data pruning methods and eight data distillation methods from the literature. A full list and their abbreviations can be found in Appendix B. We include data pruning methods from different classes, including uncertainty-based, loss-based, gradient matching, and geometry-based methods. All baselines are used for the smallest dataset (i.e., CIFAR10), but some methods do not scale to larger datasets (e.g., ImageNet). We utilize existing open source implementations and results of these methods where applicable (Park et al., 2022; Guo et al., 2022) and implement RS2 within the same code for equal comparison. We compare to existing methods which sample a static subset once before learning begins, and to methods which repeatedly sample the subset each epoch.

Training Details We use standard hyperparameters for each dataset from prior works known to achieve high accuracy. We use the same hyperparameters for all methods where applicable (e.g., batch size, training rounds, etc.). Hyperparameters individual to each baseline are set based on the best known values from prior works (Guo et al., 2022). Full hyperparameter and experiment hardware details are provided in Appendix B.

5.2. End-to-End Data Pruning Experiments

We discuss end-to-end comparisons of RS2 with data pruning baselines on supervised learning benchmarks. Results are shown in Figures 2-3 and Table 1.

Accuracy In Figure 2 we show the end-model accuracy

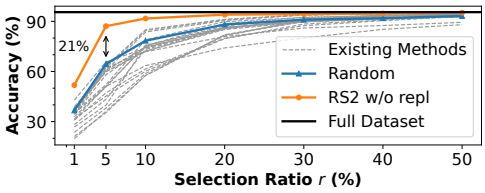

(a) CIFAR10 accuracy

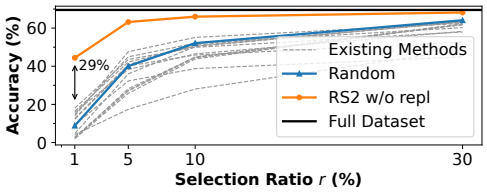

(b) ImageNet accuracy

Figure 2: Accuracy achieved by data pruning methods when training ResNet-18 on CIFAR10 and ImageNet. Repeated Sampling of Random Subsets (RS2) outperforms existing methods.

of RS2 compared to existing methods on CIFAR10 and ImageNet for varying selection ratios. We use the combined baseline methods from recent studies (Guo et al., 2022; Park et al., 2022) together with newer prototype-based data pruning methods (Sorscher et al., 2022). We include the exact accuracies for these Figures in Tables 5 and 6 in Appendix C. Here, we follow the setting proposed by these works: for all baselines we sample a static subset once before training starts. The repeated sampling of RS2 leads to accuracy improvements of at least 7% in the high compression regime ($r \leq 10\%$). For example, on CIFAR10 with 5% of the training data each epoch, RS2 achieves 87.1% accuracy while the next closest baseline reaches just 65.7%. Similar results hold on CIFAR100 and ImageNet30 (Appendix Table 7). Figure 2b shows that RS2 also outperforms existing methods for the much larger ImageNet dataset. For example, RS2 end-model accuracy with $r = 1\%$ is 46.96% while the next closest baseline trains to only 18.1%. Moreover, the end-model accuracy of RS2 is actually on par with the training on the full dataset for non-trivial selection ratios (e.g., $r = 10\%$), offering a potential practical solution to reduce the cost of training in some applications (e.g., neural architecture search) (see also runtime reductions below).

Next, we extend baselines to also perform repeated sampling. Our goal is to examine if the prior observations are attributed only to the fact that RS2 performs repeated sampling while the above baselines do not. To do so, we take all baselines and where applicable modify them as follows: For a given method M 1) if M computes a numerical example importance for each training instance, we view these values as a probability distribution over the examples and *resample* subsets according to this distribution after each round (called M-RS) and 2) if M computes example importance based on model outputs or gradients, we *recompute* example importance after each round using the current model and then choose the most important examples as the subset for the next round (called M-RC). Note that the latter set of methods (RC) are unlikely to be able to reduce training times, as they require computing the model forward pass for every example between each round, but we include their accuracy for completeness. Results on CIFAR10 (for computational considerations we do not run these methods on ImageNet) are shown in Table 1. While updating the subset for existing methods each round improves their accuracy, RS2 still reaches the highest end-model accuracy for $r \leq 10\%$. This experiment highlights the importance of *random* sampling, while the results above highlight the importance of *repeated* sampling (e.g., Random vs RS2 in Figure 2).

Table 1: Accuracy achieved by data pruning methods with per-round sampling when training ResNet-18 on CIFAR10. The training subset is update for all methods after each round, either by resampling from a static example importance distribution (RS, left) or by recomputing example importance based on model updates (RC, right). Repeated Sampling of Random Subsets (RS2) outperforms repeated sampling based on example importance. Best method bolded; Next best underlined.

Selection Ratio (r)	5%	10%	30%
Least Confidence-RS	67.6±5.1	83.4±4.9	93.7±0.4
Entropy-RS	85.2±0.9	89.8±0.4	94.4±0.3
Margin-RS	84.3±2.7	90.4±1.0	94.4±0.2
Forgetting-RS	81.9±3.1	88.3±2.4	94.0±0.1
GraNd-RS	86.2±2.1	90.1±0.9	**94.5±0.1**
CAL-RS	81.1±3.0	86.6±0.7	93.3±0.1
Craig-RS	86.7±0.8	89.8±0.2	94.3±0.1
SP-Easy-RS	84.0±4.3	88.4±0.1	93.6±0.3
CD-RC	75.2±2.2	83.1±0.7	87.5±0.2
Herding-RC	30.1±2.6	40.6±8.4	81.0±0.9
k-Center Greedy-RC	78.1±1.5	82.3±0.5	86.3±0.4
Least Confidence-RC	44.8±11.7	76.7±3.9	88.3±0.3
Entropy-RC	41.4±6.9	78.4±2.9	86.9±0.1
Margin-RC	79.7±1.4	82.8±1.4	86.8±0.2
Forgetting-RC	28.7±0.8	40.7±6.5	78.8±4.3
GraNd-RC	15.5±1.8	24.1±6.0	75.2±5.0
CAL-RC	66.7±1.7	74.5±0.8	84.8±0.4
Craig-RC	70.3±13.1	80.3±0.8	85.5±0.3
Glister-RC	72.5±0.6	81.4±0.7	86.6±0.5
RS2 w/o repl	**87.1±0.8**	**91.7±0.5**	94.3±0.2

Training Time We now study the training time of RS2 and existing methods on CIFAR10 and ImageNet. In particular, we focus on time-to-accuracy to quantify efficient training. As runtime measurements have generally not been reported in the literature, we train all methods from scratch on NVIDIA 3090 GPUs for these experiments. We use all baseline methods from Figure 2a and Figure 2b for each dataset, respectively, which do not give GPU out-of-memory. We show the time-to-accuracy on CIFAR10 in Figure 3a and on ImageNet in Figure 3b using $r = 10\%$ for both datasets. We report the total time for subset selection on CIFAR10 for

all methods in Appendix Table 8 and for baselines which utilize per-round sampling in Appendix Table 9. We also include the time-to-accuracy measurements on CIFAR10 and ImageNet for different pruning ratios in Appendix C.

Figures 3a and 3b show that RS2 provides the fastest time-to-accuracy when compared to previous data pruning methods. Note that the repeated subset selection in RS2 leads to negligible overhead compared to training on a static random subset (Figure 3) and to the total training time: For example, the total subset selection time for RS2 on CIFAR10 with $r = 10\%$ is less than one second, yet the total runtime is 750 seconds. Existing methods, however, are primarily limited by the fact that they require *pretraining* an auxiliary model on the full dataset for a few epochs in order to rank example importance. For example, on ImageNet the fastest baseline begins training after 250 minutes, yet training itself only requires 400 minutes. With $r = 1\%$, the training time drops to just 40 minutes; in this case the 250 minute overhead implies the fastest baseline is over $7\times$ slower than RS2 (250+40=290 vs 40). Even if the pretraining overhead is amortized by fixing the subset for the remaining rounds, or by resampling from the importance distribution after each round, as in our 'RS' baseline methods in Table 1, the initial overhead of these methods is still orders of magnitude higher than the total overhead of RS2 across all rounds (e.g., Table 8-9). Moreover, Figures 3a and 3b highlight the practical potential of RS2 to reduce the computational cost of training high-accuracy models: For CIFAR10, RS2 reaches 91.7% accuracy $4.3\times$ faster than standard training on the full dataset, while for ImageNet, RS2 reaches 66% accuracy $9\times$ faster than standard full dataset training.

Takeaway The above results show that RS2 outperforms existing data pruning methods with respect to end-model accuracy by up to 29%. RS2 also has the lowest subset selection overhead resulting in the best time-to-accuracy across small (CIFAR10) and large (ImageNet) datasets.

5.3. Comparison to Dataset Distillation

We also compare RS2 to dataset distillation methods which generate subsets of synthetic examples. We show the accuracy of RS2 with respect to these baselines on CIFAR10, CIFAR100, and Tiny ImageNet (rather than ImageNet30 or ImageNet for computational reasons) in Table 2. For these experiments, given the small selection ratios, we use no data augmentation when training with RS2. We also use a ConvNet rather than a ResNet to be consistent with existing dataset distillation evaluations and because such methods can be to computationally expensive to run on complex architectures. While dataset distillation methods generally outperform data pruning methods (e.g., in Table 2 a static random subset on CIFAR10 with $r = 1\%$ reaches 43.4% accuracy while data distillation methods reach up to 71.6%), they have several drawbacks. First, subsets generated by these methods are model specific, i.e., the subset must be regenerated for every model one wishes to train. The most prominent issue, however, is the computation required to generate each subset. In fact, most methods are already too expensive to run on Tiny ImageNet, even when generating only a few examples per class. The best performing method, Trajectory Matching (TM), requires 133, 317, and 433 minutes to generate the subset with 50 images per class on CIFAR10, CIFAR100, and Tiny ImageNet, respectively. In comparison, RS2 requires just seven, 33, and 187 minutes for end-to-end training in these settings. Yet RS2 outperforms TM with respect to end-model accuracy for eight of the nine selection ratio/dataset combinations in Table 2. In the extreme compression regime ($r = 0.2\%$) on Tiny ImageNet, RS2 outperforms TM by 14.7%.

5.4. Beyond Standard Supervised Learning Benchmarks

We now consider two extensions of RS2 beyond standard supervised benchmarks: We examine 1) the robustness of data pruning methods and RS2 against noisy labels and 2) explore the benefits that RS2 can have on improving time-to-accuracy when training generative pretrained transformers.

Robustness of RS2 We evaluate the robustness of data pruning methods when the operate on a training dataset with noisy labels. To do so, we randomly flip some percentage p of the labels in CIFAR10 and then run data pruning methods with these labels. We evaluate on the regular test set. Accuracy for RS2 and baseline methods when using a selection ratio of $r = 10\%$ and varying noise ratios p is shown in Appendix Table 4. For each method we report end-model accuracy/raw accuracy drop compared to $p = 0$/relative accuracy drop compared to $p = 0$ (as a percentage of the $p = 0$ accuracy). Just as for the results above on the noiseless datasets, Table 4 shows that RS2 achieves higher end-model accuracy in the presence of noisy labels compared to existing data pruning methods. For example, with 30% of the training examples mislabeled, RS2 without replacement achieves 74.4% accuracy while the next closest baseline—our modified per-round prototype-based method (SP-Easy-RS)—achieves just 63.4%. Moreover, RS2 is generally the most robust method in that it suffers the lowest relative drop in performance when presented with noisy labels. We discuss these results in more detail in Appendix C.

RS2 for Language Model Pretraining One benefit of RS2 is that it can be easily generalized to settings beyond supervised learning. In this section, we use RS2 to reduce the cost of pretraining a large GPT2 language model. We extend RS2 to this setting as follows: we repeatedly sample random subsets of text from the dataset and use this data for next token prediction (the standard GPT2 pretraining task). We train RS2 for $r \cdot 600$k iterations for $r = [0.1, 0.3]$ and

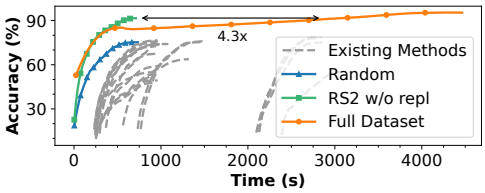

(a) CIFAR10 time-to-accuracy

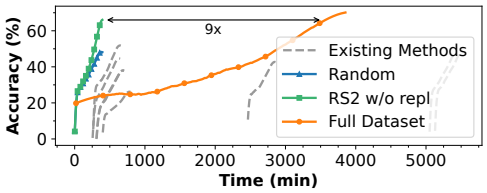

(b) ImageNet time-to-accuracy

Figure 3: Time-to-accuracy for RS2 vs. existing data pruning methods, a static random subset, and standard training on the full dataset. We use a selection ratio of $r = 10\%$. RS2 is both the fastest and highest accuracy data pruning method.

Table 2: Accuracy achieved by dataset distillation methods, RS2, and Random data pruning when training a ConvNet model. We select the specified number of images per class (Img/Cls) corresponding to the given selection ratio on the full dataset. Best method bolded. Next best underlined.

	Img/Cls	Ratio %	Random	Dataset Distillation Methods								RS2 w/ repl	Full Dataset
				DD	LD	DC	DSA	DM	CAFE	CAFE+DSA	TM		
CIFAR10	1	0.02	14.4±2.0	-	25.7±0.7	28.3±0.5	28.8±0.7	26.0±0.8	30.3±1.1	31.6±0.8	46.3±0.8	**54.7±0.5**	
	10	0.2	36.8±1.2	36.8±1.2	38.3±0.4	44.9±0.5	52.1±0.5	48.9±0.6	46.3±0.6	50.9±0.5	65.3±0.7	**72.7±0.1**	84.8±0.1
	50	1	43.4±1.0	-	42.5±0.4	53.9±0.5	60.6±0.5	63.0±0.4	55.5±0.6	62.3±0.4	71.6±0.2	**76.5±0.3**	
CIFAR100	1	0.2	4.2±0.3	-	11.5±0.4	12.8±0.3	13.9±0.3	11.4±0.3	12.9±0.3	14.0±0.3	24.3±0.3	**37.4±0.4**	
	10	2	14.6±0.5	-	-	25.2±0.3	32.3±0.3	29.7±0.3	27.8±0.3	31.5±0.2	40.1±0.4	**43.9±0.4**	56.2±0.3
	50	10	30.0±0.4	-	-	-	42.8±0.4	43.6±0.4	37.9±0.3	42.9±0.2	**47.7±0.2**	44.6±0.3	
Tiny ImageNet	1	0.2	1.4±0.1	-	-	-	-	3.9±0.2	-	-	8.8±0.3	**23.5±0.2**	
	10	2	5.0±0.2	-	-	-	-	12.9±0.4	-	-	23.2±0.2	**27.4±0.1**	37.6±0.4
	50	10	15.0±0.4	-	-	-	-	24.1±0.3	-	-	28.0±0.3	**28.6±0.4**	

compare to training with the full dataset for 600k iterations (recall the connection between RS2 and early stopping). We also compare RS2 to random data pruning, i.e., training for $r \cdot 600$k iterations on a static fraction r of the full dataset selected once before learning begins. We are not aware of existing data pruning methods being evaluated in this setting and present these results as an initial baseline.

Results of pretraining GPT2 on OpenWebText according to different strategies are shown Table 3 in the Appendix. We report accuracy (higher is better) and perplexity (lower is better) on the LAMBADA (Paperno et al., 2016) benchmark as well as perplexity on WikiText103 (Merity et al., 2016). Observe that RS2 leads to better model quality but not cost compared to a static random sample. Moreover, we see that RS2 leads to near matching accuracy and perplexity compared to training using the full dataset for $r = 30\%$. This result again highlights the practical potential of RS2 to enable faster and cheaper training, hyperparameter tuning, or neural arcitecture search for large language model pretraining, currently one of the most expensive and time consuming training paradigms in machine learning.

6. Discussion and Conclusion

We end by discussing the limitations of RS2 before concluding and presenting future directions.

RS2 Limitations In this work, we focused on minimizing time-to-accuracy when training over a large, labeled dataset. When the full dataset is not labeled, or when the primary metric of interest is not time-to-accuracy, RS2 may not outperform existing methods. In particular, RS2 is likely to be a weaker baseline when the goal is to minimize the cost of labeling examples for training by selecting a subset from a large, unlabeled dataset. We refer the reader to active learning based methods (Park et al., 2022; Ren et al., 2021) for this regime. The assumption of labels for the full dataset is not unique to our work, however, as most recent methods for reducing time-to-accuracy utilize the labels of the full dataset S to create the subset S' (Toneva et al., 2018; Mirzasoleiman et al., 2020; Sachdeva et al., 2021; Paul et al., 2021; Killamsetty et al., 2021a) for training.

Conclusion and Future Work Through extensive experiments, we have shown that training on random subsets repeatedly sampled (RS2) from a large dataset results in reduced runtime and higher end-model accuracy when compared to existing data pruning and distillation methods. While the impressive performance of RS2 may provide a practical solution for reducing time-to-accuracy, e.g., for hyperparameter tuning or neural architecture search, we also hope that our findings serve as a baseline for future research to minimize time-to-accuracy through data subset selection. Specifically, we are excited for future work focused on the following question: How can we further close the gap between RS2 and training on the full dataset? Interesting sub directions to answering this question include: 1) further study of importance sampling-based methods for reducing time-to-accuracy and 2) improving the subset training procedure (independent of the method) to benefit the end-model accuracy. The key issue with the latter is that training on a subset results in fewer total SGD iterations when com-

pared to training on the full dataset for the same number of rounds. Can we overcome this limitation of data pruning when training with SGD without eliminating the runtime benefits? We encourage new research into these questions to enable further reductions in time-to-accuracy.

Acknowledgements

We would like to thank the anonymous reviewers for their constructive comments on our paper. This work was supported by DARPA under grant ASKEM HR001122S0005. The U.S. Government is authorized to reproduce and distribute reprints for Governmental purposes notwithstanding any copyright notation thereon. Any opinions, findings, and conclusions or recommendations expressed in this material are those of the authors and do not necessarily reflect the views, policies, or endorsements, either expressed or implied, of DARPA or the U.S. Government. This work is also supported with funding from the Wisconsin Alumni Research Foundation. Amin Karbasi acknowledges funding in direct support of this work from NSF (IIS-1845032), ONR (N00014- 19-1-2406), and the AI Institute for Learning-Enabled Optimization at Scale (TILOS).

References

Agarwal, S., Arora, H., Anand, S., and Arora, C. Contextual diversity for active learning. In *ECCV*, pp. 137–153. Springer, 2020.

Ayed, F. and Hayou, S. Data pruning and neural scaling laws: fundamental limitations of score-based algorithms. *arXiv preprint arXiv:2302.06960*, 2023.

Bachem, O., Lucic, M., and Krause, A. Coresets for nonparametric estimation-the case of dp-means. In *ICML*, pp. 209–217. PMLR, 2015.

Bateni, M., Bhaskara, A., Lattanzi, S., and Mirrokni, V. S. Distributed balanced clustering via mapping coresets. In *NIPS*, pp. 2591–2599, 2014.

Bohdal, O., Yang, Y., and Hospedales, T. Flexible dataset distillation: Learn labels instead of images. *arXiv preprint arXiv:2006.08572*, 2020.

Brown, T., Mann, B., Ryder, N., Subbiah, M., Kaplan, J. D., Dhariwal, P., Neelakantan, A., Shyam, P., Sastry, G., Askell, A., et al. Language models are few-shot learners. *Advances in neural information processing systems*, 33: 1877–1901, 2020.

Cazenavette, G., Wang, T., Torralba, A., Efros, A. A., and Zhu, J.-Y. Dataset distillation by matching training trajectories. In *Proceedings of the IEEE/CVF Conference on Computer Vision and Pattern Recognition*, pp. 4750–4759, 2022.

Chen, Y., Welling, M., and Smola, A. Super-samples from kernel herding. *The Twenty-Sixth Conference Annual Conference on Uncertainty in Artificial Intelligence*, 2010.

Chiu, C.-C., Sainath, T. N., Wu, Y., Prabhavalkar, R., Nguyen, P., Chen, Z., Kannan, A., Weiss, R. J., Rao, K., Gonina, E., et al. State-of-the-art speech recognition with sequence-to-sequence models. In *2018 IEEE international conference on acoustics, speech and signal processing (ICASSP)*, pp. 4774–4778. IEEE, 2018.

Cotter, A., Shamir, O., Srebro, N., and Sridharan, K. Better mini-batch algorithms via accelerated gradient methods. *Advances in neural information processing systems*, 24, 2011.

Dasgupta, S., Hsu, D., Poulis, S., and Zhu, X. Teaching a black-box learner. In *ICML*. PMLR, 2019.

De Sa, C. M. Random reshuffling is not always better. In Larochelle, H., Ranzato, M., Hadsell, R., Balcan, M., and Lin, H. (eds.), *Advances in Neural Information Processing Systems*, volume 33, pp. 5957–5967. Curran Associates, Inc., 2020. URL https://proceedings.neurips.cc/paper_files/paper/2020/file/42299f06ee419aa5d9d07798b56779e2-Paper.pdf.

Dekel, O., Gilad-Bachrach, R., Shamir, O., and Xiao, L. Optimal distributed online prediction using mini-batches. *Journal of Machine Learning Research*, 13(1), 2012.

Deng, Z. and Russakovsky, O. Remember the past: Distilling datasets into addressable memories for neural networks. *arXiv preprint arXiv:2206.02916*, 2022.

Dosovitskiy, A., Beyer, L., Kolesnikov, A., Weissenborn, D., Zhai, X., Unterthiner, T., Dehghani, M., Minderer, M., Heigold, G., Gelly, S., et al. An image is worth 16x16 words: Transformers for image recognition at scale. *arXiv preprint arXiv:2010.11929*, 2020.

Ducoffe, M. and Precioso, F. Adversarial active learning for deep networks: a margin based approach. *arXiv preprint arXiv:1802.09841*, 2018.

Ghadimi, S. and Lan, G. Accelerated gradient methods for nonconvex nonlinear and stochastic programming. *Mathematical Programming*, 156(1-2):59–99, 2016.

Gokaslan, A. and Cohen, V. Openwebtext corpus. http://Skylion007.github.io/OpenWebTextCorpus, 2019.

Guo, C., Zhao, B., and Bai, Y. Deepcore: A comprehensive library for coreset selection in deep learning. In

Database and Expert Systems Applications: 33rd International Conference, DEXA 2022, Vienna, Austria, August 22–24, 2022, Proceedings, Part I, pp. 181–195. Springer, 2022.

Haochen, J. and Sra, S. Random shuffling beats sgd after finite epochs. In *International Conference on Machine Learning*, pp. 2624–2633. PMLR, 2019.

Hardt, M., Recht, B., and Singer, Y. Train faster, generalize better: Stability of stochastic gradient descent. In Balcan, M. F. and Weinberger, K. Q. (eds.), *Proceedings of The 33rd International Conference on Machine Learning*, volume 48 of *Proceedings of Machine Learning Research*, pp. 1225–1234, New York, New York, USA, 20–22 Jun 2016. PMLR. URL https://proceedings.mlr.press/v48/hardt16.html.

He, K., Zhang, X., Ren, S., and Sun, J. Deep residual learning for image recognition. In *Proceedings of the IEEE conference on computer vision and pattern recognition*, pp. 770–778, 2016.

Hendrycks, D., Mazeika, M., Kadavath, S., and Song, D. Using self-supervised learning can improve model robustness and uncertainty. *Advances in neural information processing systems*, 32, 2019.

Iyer, R., Khargoankar, N., Bilmes, J., and Asanani, H. Submodular combinatorial information measures with applications in machine learning. In *Algorithmic Learning Theory*, pp. 722–754. PMLR, 2021.

Kaufmann, M., Zhao, Y., Shumailov, I., Mullins, R., and Papernot, N. Efficient adversarial training with data pruning. *arXiv preprint arXiv:2207.00694*, 2022.

Killamsetty, K., Durga, S., Ramakrishnan, G., De, A., and Iyer, R. Grad-match: Gradient matching based data subset selection for efficient deep model training. In *ICML*, pp. 5464–5474, 2021a.

Killamsetty, K., Sivasubramanian, D., Ramakrishnan, G., and Iyer, R. Glister: Generalization based data subset selection for efficient and robust learning. In *Proceedings of the AAAI Conference on Artificial Intelligence*, 2021b.

Killamsetty, K., Zhao, X., Chen, F., and Iyer, R. Retrieve: Coreset selection for efficient and robust semi-supervised learning. *arXiv preprint arXiv:2106.07760*, 2021c.

Kim, J.-H., Kim, J., Oh, S. J., Yun, S., Song, H., Jeong, J., Ha, J.-W., and Song, H. O. Dataset condensation via efficient synthetic-data parameterization. In *International Conference on Machine Learning*, pp. 11102–11118. PMLR, 2022.

Krizhevsky, A., Hinton, G., et al. Learning multiple layers of features from tiny images. 2009.

Lan, G. An optimal method for stochastic composite optimization. *Mathematical Programming*, 133(1-2):365–397, 2012.

Lee, S., Chun, S., Jung, S., Yun, S., and Yoon, S. Dataset condensation with contrastive signals. In *International Conference on Machine Learning*, pp. 12352–12364. PMLR, 2022.

Liu, E. Z., Haghgoo, B., Chen, A. S., Raghunathan, A., Koh, P. W., Sagawa, S., Liang, P., and Finn, C. Just train twice: Improving group robustness without training group information. In *ICML*, pp. 6781–6792, 2021.

Loshchilov, I. and Hutter, F. Sgdr: Stochastic gradient descent with warm restarts. *arXiv preprint arXiv:1608.03983*, 2016.

Lu, Y., Guo, W., and De Sa, C. M. Grab: Finding provably better data permutations than random reshuffling. *Advances in Neural Information Processing Systems*, 35: 8969–8981, 2022.

Merity, S., Xiong, C., Bradbury, J., and Socher, R. Pointer sentinel mixture models. *arXiv preprint arXiv:1609.07843*, 2016.

Mindermann, S., Brauner, J. M., Razzak, M. T., Sharma, M., Kirsch, A., Xu, W., Höltgen, B., Gomez, A. N., Morisot, A., Farquhar, S., et al. Prioritized training on points that are learnable, worth learning, and not yet learnt. In *International Conference on Machine Learning*, pp. 15630–15649. PMLR, 2022.

Mirzasoleiman, B., Bilmes, J., and Leskovec, J. Coresets for data-efficient training of machine learning models. In *ICML*. PMLR, 2020.

Munteanu, A., Schwiegelshohn, C., Sohler, C., and Woodruff, D. P. On coresets for logistic regression. In *NeurIPS*, 2018.

Nesterov, Y. *Introductory lectures on convex optimization: A basic course*, volume 87. Springer Science & Business Media, 2003.

Nesterov, Y. E. A method of solving a convex programming problem with convergence rate o\bigl(k^2\bigr). In *Doklady Akademii Nauk*, volume 269, pp. 543–547. Russian Academy of Sciences, 1983.

Nikolakakis, K. E., Karbasi, A., and Kalogerias, D. Select without fear: Almost all mini-batch schedules generalize optimally. *arXiv preprint arXiv:2305.02247*, 2023.

OpenAI. Gpt-4 technical report, 2023.

Paperno, D., Kruszewski, G., Lazaridou, A., Pham, Q. N., Bernardi, R., Pezzelle, S., Baroni, M., Boleda, G., and Fernández, R. The lambada dataset: Word prediction requiring a broad discourse context, 2016.

Park, D., Papailiopoulos, D., and Lee, K. Active learning is a strong baseline for data subset selection. In *Has it Trained Yet? NeurIPS 2022 Workshop*, 2022. URL https://openreview.net/forum?id=PAgpyQ5rGS.

Paul, M., Ganguli, S., and Dziugaite, G. K. Deep learning on a data diet: Finding important examples early in training. *arXiv preprint arXiv:2107.07075*, 2021.

Radford, A., Wu, J., Child, R., Luan, D., Amodei, D., and Sutskever, I. Language models are unsupervised multitask learners. 2019.

Radford, A., Kim, J. W., Hallacy, C., Ramesh, A., Goh, G., Agarwal, S., Sastry, G., Askell, A., Mishkin, P., Clark, J., et al. Learning transferable visual models from natural language supervision. In *International conference on machine learning*, pp. 8748–8763. PMLR, 2021.

Ren, P., Xiao, Y., Chang, X., Huang, P.-Y., Li, Z., Gupta, B. B., Chen, X., and Wang, X. A survey of deep active learning. *ACM computing surveys (CSUR)*, 54(9):1–40, 2021.

Russakovsky, O., Deng, J., Su, H., Krause, J., Satheesh, S., Ma, S., Huang, Z., Karpathy, A., Khosla, A., Bernstein, M., Berg, A. C., and Fei-Fei, L. ImageNet Large Scale Visual Recognition Challenge. *IJCV*, 2015.

Sachdeva, N., Wu, C.-J., and McAuley, J. Svp-cf: Selection via proxy for collaborative filtering data. *arXiv preprint arXiv:2107.04984*, 2021.

Sener, O. and Savarese, S. Active learning for convolutional neural networks: A core-set approach. In *ICLR*, 2018.

Sorscher, B., Geirhos, R., Shekhar, S., Ganguli, S., and Morcos, A. Beyond neural scaling laws: beating power law scaling via data pruning. *Advances in Neural Information Processing Systems*, 35:19523–19536, 2022.

Toneva, M., Sordoni, A., des Combes, R. T., Trischler, A., Bengio, Y., and Gordon, G. J. An empirical study of example forgetting during deep neural network learning. In *ICLR*, 2018.

Wang, K., Zhao, B., Peng, X., Zhu, Z., Yang, S., Wang, S., Huang, G., Bilen, H., Wang, X., and You, Y. Cafe: Learning to condense dataset by aligning features. In *Proceedings of the IEEE/CVF Conference on Computer Vision and Pattern Recognition*, pp. 12196–12205, 2022.

Wang, T., Zhu, J.-Y., Torralba, A., and Efros, A. A. Dataset distillation. *arXiv preprint arXiv:1811.10959*, 2018.

Wang, W. and Srebro, N. Stochastic nonconvex optimization with large minibatches, 2019.

Welling, M. Herding dynamical weights to learn. In *Proceedings of the 26th Annual International Conference on Machine Learning*, pp. 1121–1128, 2009.

Yu, R., Liu, S., and Wang, X. Dataset distillation: A comprehensive review. *arXiv preprint arXiv:2301.07014*, 2023.

Zhao, B. and Bilen, H. Dataset condensation with differentiable siamese augmentation. In *International Conference on Machine Learning*, 2021.

Zhao, B. and Bilen, H. Dataset condensation with distribution matching. In *Proceedings of the IEEE/CVF Winter Conference on Applications of Computer Vision*, pp. 6514–6523, 2023.

Zhao, B., Mopuri, K. R., and Bilen, H. Dataset condensation with gradient matching. In *International Conference on Learning Representations*, 2021. URL https://openreview.net/forum?id=mSAKhLYLSsl.

Appendix

A. A Motivating Experiment

We have shown in the main body of the paper that Repeated Sampling of Random Subsets (RS2) allows for faster training and more accurate models when compared to existing data pruning and dataset distillation techniques. In this section, we discuss a simple experiment that helped motivate our work.

Existing data pruning methods are primarily based on the intuition that a small subset S' of 'difficult' (Toneva et al., 2018; Paul et al., 2021) (or sometimes 'easy' (Sorscher et al., 2022)) examples contained in the full dataset S are close to (far from) the decision boundary and thus likely to be the most informative for learning. During our initial investigation into data pruning methods, we empirically studied this intuition. Calculating the distance between a training example and the decision boundary, however, can be challenging because the decision boundary is not known until training completes, and because the location of the decision boundary in high dimensional space can be computationally intensive to compute. Thus, we consider the following proxy measurement: To decide whether a training example x is close to the decision boundary, we find the nearest neighbor (e.g., L_2 distance) from the full dataset and check whether it has the same label as x. If not, then the decision boundary in the input feature space must be between the two points (i.e., they are 'close' to the boundary).

We evaluated the above proxy measurement for all examples in the CIFAR10 dataset to decide whether each one was close to the decision boundary. Surprisingly, we found that the nearest neighbor for 65% of the training examples had a different label than the example itself. In other words, in the raw feature space, this experiment provides some evidence that a majority of examples may be needed for learning the final decision boundary. This observation motivates RS2 as a strong data pruning baseline because it satisfies two desired properties: 1) it maximizes overall data coverage by periodically resampling the subset and 2) it provides representative examples from the dataset without overfitting. We remark that a majority of points are unlikely to be on the decision boundary if we first encode the input examples x into a more semantically meaningful feature space. Learning such an encoding, however, requires first learning a decision boundary over the raw features and must be done during the model training itself. We leave a detailed study of this experiment, and the implications of this observation on selecting hard/easy examples for importance-sampling based data pruning to future work.

B. Additional Experimental Setup

We expand on the experimental setup described in Section 5.1 of the main body of the paper.

B.1. Data Pruning Baselines

We consider the following 22 data pruning baselines. We refer the reader to existing studies for more detailed descriptions of these methods (Guo et al., 2022).

1. Random: standard baseline; sample a static random subset of the dataset once before training
2. Contextual Diversity (CD) (Agarwal et al., 2020)
3. Herding (Welling, 2009; Chen et al., 2010)
4. K-Center Greedy (Sener & Savarese, 2018)
5. Least Confidence (Sachdeva et al., 2021)
6. Entropy (Sachdeva et al., 2021)
7. Margin (Sachdeva et al., 2021)
8. Forgetting (Toneva et al., 2018)
9. GraNd (Paul et al., 2021)
10. Contrastive Active Learning (CAL) (Liu et al., 2021)
11. Craig (Mirzasoleiman et al., 2020)
12. GradMatch (Killamsetty et al., 2021a)
13. Glister (Killamsetty et al., 2021b)
14. Facility Location (FL) (Iyer et al., 2021)

15. GraphCut (Iyer et al., 2021)
16. Active Learning with confidence-based example informativeness (AL (Conf)) (Park et al., 2022)
17. Active Learning with loss-based example informativeness (AL (LL)) (Park et al., 2022)
18. Active Learning with margin-based example informativeness (AL (Margin)) (Park et al., 2022)
19. Self-supervised prototypes with easy examples (SSP-Easy) (Sorscher et al., 2022)
20. Self-supervised prototypes with hard examples (SSP-Hard) (Sorscher et al., 2022)
21. Supervised prototypes with easy examples (SP-Easy) (Sorscher et al., 2022)
22. Supervised prototypes with hard examples (SP-Hard) (Sorscher et al., 2022)

B.2. Dataset Distillation Baselines

We compare against the following eight dataset distillation methods.

1. Dataset Distillation (DD) (Wang et al., 2018)
2. Flexible Dataset Distillation (LD) (Bohdal et al., 2020)
3. Dataset Condensation (DC) (Zhao et al., 2021)
4. Differentiable Siamese Augmentation (DSA) (Zhao & Bilen, 2021)
5. Distribution Matching (DM) (Zhao & Bilen, 2023)
6. Aligning Features (CAFE) (Wang et al., 2022)
7. Aligning Features + Differentiable Siamese Augmentation (CAFE+DSA) (Wang et al., 2022)
8. Trajectory Matching (TM) (Cazenavette et al., 2022)

B.3. Additional Training Details

For all experiments (except GPT2 due to cost considerations) we conduct three runs using different random seeds and report the average accuracy and runtime. We include additional details on the hyperparameters and hardware used below.

Hyperparameters We use the following hyperparameters for our experiments: For CIFAR10 and CIFAR100 experiments, we use SGD as the optimizer with batch size 128, initial learning rate 0.1, a cosine decay learning rate schedule, momentum 0.9, weight decay 0.0005, and 200 training epochs. For data augmentation, we apply random cropping and horizontal flipping with four-pixel padding on the 32×32 training images. For ImageNet30 and ImageNet, we use the same hyerparameters as above except for a larger batch size on ImageNet (256). We also use different data augmentation: training images are randomly resized and cropped to 224×224 with random horizontal flipping. Further details can be found in the source code.

Hardware Setup We run image classification experiments on a university cluster with job isolation and NVIDIA RTX 3090 GPUs. We run GPT2 experiments using AWS P3 GPU instances with eight NVIDIA V100 GPUs (as GPT2 experiments require more compute power). Utilizing the former allows us to reduce the cost of our experiments (e.g., compared to training entirely using AWS), but introduces the potential for increased variance compared to training with completely dedicated hardware—Even though all experiments run with exclusive access to one GPU and a set of CPU cores, cluster load can influence runtime measurements. We observe small variance across multiple runs of the same experiment on small datasets (e.g., on CIFAR10 the three run standard deviation is generally less than one percent of the total runtime), but larger variance on ImageNet, likely do to an increased load on the shared file system and longer experiment runtimes. As such, we calculate the runtime of each method on ImageNet as follows: We calculate the minimum time per mini-batch using all runs across *all* methods, and then use this value to compute individual method runtimes by multiplying by the total number of batches during training and adding any necessary overheads for subset selection. More specifically, we have: the total runtime of any method $T_{\text{total}} = T_{\text{total\_subset\_selection}} + T_{\text{total\_training\_time}}$ with $T_{\text{total\_training\_time}} = T_{\text{global\_minimum\_batch\_runtime}} \times$ total_number_of_batches. Note that this means runtimes differ only due to subset selection overhead as expected (once a subset has been selected, all methods train on the same number of examples per round using the same hardware, and thus should have the same per round training time). Furthermore, we calculate $T_{\text{total\_subset\_selection}}$ as the minimum subset selection time observed across three runs of each method. The above runtime calculation allows us to minimize the affect of cluster noise on our experiments and ensure a fair comparison for the ImageNet time-to-accuracy reported in the paper.

Table 3: Zero-shot results of GPT2 pretrained using RS2, a static random subset, and the full dataset. We report accuracy (ACC; higher is better) and perplexity (PPL; lower is better).

Method	Selection Ratio (r)	2023 AWS Training Cost	Task LAMBADA (ACC ↑)	Task LAMBADA (PPL ↓)	Task WikiText103 (PPL ↓)
Random	10%	$520	43.37	45.02	53.36
Random	30%	$1,560	44.63	41.99	46.44
RS2 w/ repl	10%	$520	44.42	41.67	45.72
RS2 w/ repl	30%	$1,560	45.29	40.51	42.58
Full Dataset	-	$5,200	46.61	40.30	40.55

Table 4: Accuracy achieved by different data pruning methods when training ResNet-18 on the CIFAR10 dataset with p percent of the train set labels randomly flipped (noise ratio). Data pruning methods use a selection ratio of 10%. We test on the normal test set. We report raw end-model accuracy/accuracy drop compared to $p = 0$/relative accuracy drop compared to $p = 0$ (as a percentage of the $p = 0$ accuracy). Best method (highest accuracy) bolded; Next best underlined. Most robust method (lowest relative accuracy drop) starred.

Noise Ratio	10%	30%	50%
Random	50.7±1.0/27.7/35.4	40.9±2.3/37.5/47.8	37.2±1.1/41.2/52.6
CD	31.2±3.9/27.6/47.0	30.3±0.6/28.5/48.4	29.7±2.9/29.1/49.5
Herding	15.9±2.2/47.6/74.9	17.1±1.1/46.4/73.1	16.1±1.8/47.4/74.7
K-Center Greedy	41.6±1.7/33.6/44.6	33.1±0.7/42.1/56.0	31.1±0.4/44.1/58.6
Least Confidence	27.4±0.7/30.2/52.4	25.2±2.1/32.4/56.2	24.5±2.6/33.1/57.5
Entropy	26.9±4.2/30.7/53.2	24.9±3.7/32.7/56.8	23.3±2.0/34.3/59.5
Margin	29.2±2.2/44.0/60.1	27.4±2.2/45.8/62.6	28.5±3.3/44.7/61.0
Forgetting	47.5±1.6/31.5/39.9	48.3±1.7/30.7/38.9	49.0±1.6/30.0/37.9
GraNd	34.5±3.2/40.9/54.3	49.4±5.6/26.0/34.5	60.0±1.3/15.4/20.4*
CAL	45.4±2.5/26.4/36.8	39.9±1.2/31.9/44.4	35.5±0.4/36.3/50.5
Craig	50.3±0.7/9.9/16.5	39.5±0.8/20.7/34.4	37.3±1.5/22.9/38.0
Glister	49.8±2.5/25.9/34.2	40.1±1.5/35.6/47.1	37.9±1.5/37.8/50.0
GraphCut	50.6±1.4/23.4/31.7	42.0±0.7/32.0/43.2	37.7±1.1/36.3/49.0
FL	50.4±2.1/24.3/32.5	41.6±0.8/33.1/44.3	36.8±0.7/37.9/50.7
AL (Conf)	53.5±3.1/30.1/36.0	47.1±0.9/36.5/43.7	37.2±1.4/46.4/55.5
AL (LL)	57.1±0.4/27.9/32.8	45.1±1.8/39.9/46.9	38.2±0.6/46.8/55.1
AL (Margin)	57.6±0.5/26.9/31.8	46.1±1.2/38.4/45.4	36.9±1.0/47.6/56.3
SSP-Easy	51.1±1.5/20.9/29.0	40.7±1.9/31.3/43.4	36.7±1.0/35.3/49.1
SSP-Hard	50.4±0.3/23.9/32.2	40.9±1.5/33.4/44.9	36.3±1.9/38.0/51.2
SP-Easy	48.4±2.4/23.9/33.0	40.0±0.4/32.3/44.6	37.7±1.0/34.6/47.8
SP-Hard	47.5±2.4/26.6/35.9	39.7±1.3/34.4/46.4	34.3±2.0/39.8/53.7
SP-Easy-RS	74.2±0.6/14.2/16.0	63.4±1.0/25.0/28.3	57.8±0.7/30.6/34.7
RS2 w/ repl	77.5±1.0/12.2/13.6*	69.9±0.4/19.8/22.1	64.6±1.5/25.1/28.0
RS2 w/ repl (stratified)	76.1±0.5/13.7/15.3	68.7±0.6/21.1/23.5	65.0±1.4/24.8/27.7
RS2 w/o repl	**78.7±0.8/13.0/14.1**	**74.4±0.6/17.3/18.9***	**69.0±0.9/22.7/24.8**

C. Additional Experimental Results

Here we include additional evaluation result comparing Repeated Sampling of Random Subsets (RS2) to existing data pruning and dataset distillation methods. These results extend those presented in Section 5 of the main paper. We briefly discuss each result (table) in turn and how it connects to the arguments made in Section 5.

First, in Table 3 we show the results of pretraining GPT2 on OpenWebText according to different data pruning strategies. Observe that RS2 leads to better model quality but not cost compared to training with a static random sample of the full dataset. Moreover, training with RS2 also leads to end-model quality comparable to training on the full dataset when using a selection ratio $r = 30\%$. See Section 5.4 for more details and discussion.

In Table 4 we show the robustness of RS2 and existing data pruning methods against noisy labels. We include existing methods which sample static subsets, as well as our modified version of the recent prototype-based data pruning method which utilizes repeated subset selection between each round (SP-Easy-RS) (see Section 5.2). As discussed in Section 5.4 in the main paper, we evaluate the robustness of data pruning methods as follows: We randomly flip some percentage p of the labels in CIFAR10 and then run data pruning methods with these labels. We use a subset selection ratio $r = 10\%$ for all methods and evaluate on the regular test set. For each method we report end-model accuracy/raw accuracy drop compared to $p = 0$/relative accuracy drop compared to $p = 0$ (as a percentage of the $p = 0$ accuracy). Table 4 shows that RS2 achieves higher end-model accuracy than existing data pruning methods in the presence of noisy labels. RS2 is also the most robust

Table 5: Accuracy achieved by different data pruning methods when training ResNet-18 on CIFAR10 for different subset selection sizes. Best method bolded; Next best underlined.

Selection Ratio (r)	1%	5%	10%	20%	30%	40%	50%	100%
Random	36.7±1.7	64.5±1.1	78.4±0.9	88.1±0.5	91.0±0.3	91.9±0.2	93.2±0.3	95.5±0.2
CD	23.6±1.9	38.1±2.2	58.8±2.0	81.3±2.5	90.8±0.5	93.3±0.4	94.3±0.2	95.5±0.2
Herding	34.8±3.3	51.0±3.1	63.5±3.4	74.1±2.5	80.1±2.2	85.2±0.9	88.0±1.1	95.5±0.2
K-Center Greedy	31.1±1.2	51.4±2.1	75.2±1.7	87.3±1.0	91.2±0.6	92.2±0.5	93.8±0.5	95.5±0.2
Least Confidence	19.8±2.2	36.2±1.9	57.6±3.1	81.9±2.2	90.3±0.4	93.1±0.5	94.5±0.1	95.5±0.2
Entropy	21.1±1.3	35.3±3.0	57.6±2.8	81.9±0.4	89.8±1.6	93.2±0.2	94.4±0.3	95.5±0.2
Margin	28.2±1.0	43.4±3.3	73.2±1.3	85.5±0.9	91.3±0.5	93.6±0.3	94.5±0.2	95.5±0.2
Forgetting	35.2±1.6	52.1±2.2	79.0±1.0	89.8±0.9	92.3±0.4	93.6±0.4	93.8±0.3	95.5±0.2
GraNd	26.7±1.3	39.8±2.3	75.4±1.2	88.6±0.6	92.4±0.4	93.3±0.5	94.2±0.4	95.5±0.2
CAL	37.8±2.0	60.0±1.4	71.8±1.0	80.9±1.1	86.0±1.9	87.5±0.8	89.4±0.6	95.5±0.2
Craig	31.7±1.1	45.2±2.9	60.2±4.4	79.6±3.1	88.4±0.5	90.8±1.4	93.3±0.6	95.5±0.2
GradMatch	30.8±1.0	47.2±0.7	61.5±2.4	79.9±2.6	87.4±2.0	90.4±1.5	92.9±0.6	95.5±0.2
Glister	32.9±2.4	50.7±1.5	75.7±1.0	86.3±0.9	90.1±0.7	91.5±0.5	93.3±0.6	95.5±0.2
FL	38.9±1.4	60.8±2.5	74.7±1.3	85.6±1.9	91.4±0.4	93.2±0.3	93.9±0.2	95.5±0.2
GraphCut	42.8±1.3	65.7±1.2	74.0±1.5	86.3±0.9	90.2±0.5	91.5±0.4	93.8±0.5	95.5±0.2
AL (Conf)	35.2±1.5	60.6±3.1	83.6±0.7	90.5±0.4	93.8±0.4	94.8±0.3	95.1±0.3	95.5±0.2
AL (LL)	37.5±4.3	63.1±2.0	85.0±0.9	91.2±0.7	93.8±0.6	94.4±0.5	95.0±0.4	95.5±0.2
AL (Margin)	36.7±0.8	62.2±1.1	84.5±0.7	91.0±0.5	93.9±0.4	94.5±0.3	**95.3±0.2**	95.5±0.2
SSP-Easy	35.6±1.7	62.1±1.2	72.0±0.8	85.9±0.4	90.0±0.2	91.5±0.4	92.7±0.0	95.5±0.2
SSP-Hard	34.2±1.1	58.0±2.4	74.3±1.7	86.1±1.3	90.3±0.4	91.9±0.3	93.3±0.2	95.5±0.2
SP-Easy	37.1±1.4	59.8±0.5	72.3±2.9	85.1±1.0	89.6±0.2	91.6±0.2	92.7±0.2	95.5±0.2
SP-Hard	35.0±0.7	60.9±1.8	74.1±1.1	86.3±0.3	89.8±0.6	91.5±0.3	93.0±0.3	95.5±0.2
RS2 w/ repl	51.1±3.5	86.7±0.8	89.7±0.2	93.5±0.3	94.2±0.1	94.6±0.2	95.1±0.2	95.5±0.2
RS2 w/ repl (stratified)	51.1±4.5	86.6±0.5	89.8±0.4	93.4±0.1	**94.5±0.1**	**94.8±0.1**	95.1±0.3	95.5±0.2
RS2 w/o repl	**51.8±2.0**	**87.1±0.8**	**91.7±0.5**	**94.0±0.5**	94.3±0.2	94.7±0.1	95.2±0.1	95.5±0.2

method (lowest relative accuracy drop) when the noise ratio is 10% and 30%. Interestingly, the GraNd baseline actually gets better as the noise ratio increases. While surprising, the overall end-model quality of GraNd is still limited, however, as the GraNd accuracy begins to decrease again as the noise increases beyond 50% and all noise ratios result in lower accuracy than training on clean data. We leave a detailed study of these observations and robust data pruning methods for future work.

In Tables 5-6 we show the end-model accuracy of RS2 and existing data pruning methods for varying selection ratios on CIFAR10 and ImageNet respectively. The numbers in these tables were used to create Figure 2 in the main body of the paper. Recall from the discussion of Figure 2 in Section 5.2 that we use the combined baseline methods from recent studies (Park et al., 2022; Guo et al., 2022) together with newer prototype-based data pruning methods (Sorscher et al., 2022). Recall also that for these tables, we use the setting proposed by these works: for all baselines, we sample a static subset once before training starts. We use all baseline methods for CIFAR10, but some methods do not scale to the larger ImageNet dataset. We show in Table 8 that active learning already takes more than eight hours for subset selection in some settings on CIFAR10 and we are not aware of a scalable implementation of prototype-based methods that would allow for training on ImageNet. As in Figure 2, Tables 5-6 show that the repeated sampling of RS2 leads to accuracy improvements compared to existing data pruning methods which sample a static subset (see discussion in Section 5.2). Interestingly, while RS2 generally outperforms existing methods in the high compression regime ($r \leq 10\%$), for extreme compression ratios, like $r = 0.1\%$ on ImageNet, we find RS2 to be inferior to existing methods. We hypothesize that this occurs because in these extreme regimes, only a few examples are shown to the model for each class and these examples likely have large variance when using repeated random sampling coupled with data augmentation. In this setting, it may be best to select a static subset of only the easiest examples as highlighted in recent work (Sorscher et al., 2022), however the significance of this regime is debatable given the low end-model accuracy of all methods. Improving the performance in these regimes is of interest for future work.

In Table 7, we include additional end-model accuracy results for RS2 and existing data pruning methods on two datasets, CIFAR100 and ImageNet30, not included in the main paper due to space considerations. For these experiments, we include a representative set of baseline methods which sample static subsets, together with our modified version of the recent prototype-based data pruning method which utilizes repeated subset selection between each round (SP-Easy-RS) (see Section 5.2). Thus, Table 7 extends the end-model accuracy results presented previously for CIFAR10 and ImageNet in Figure 2 and Tables 1, 5, and 6. Observe that RS2 also outperforms existing methods on these datasets. For example, in the high compression regime ($r = 10\%$), RS2 without replacement reaches 73% accuracy on CIFAR100, while the best baseline method, our per-round prototype-based data pruning method reaches only 66%. Existing methods which sample

Table 6: Accuracy achieved by different data pruning methods when training ResNet-18 on ImageNet for different subset selection sizes. Repeatedly Sampling Random Subsets (RS2) considerably outperforms existing methods for realistic selection ratios. Best method bolded; Next best underlined.

Select Ratio (r)	0.1%	0.5%	1%	5%	10%	30%	100%
Random	0.76±0.01	3.78±0.14	8.85±0.46	40.09±0.21	52.1±0.22	64.11±0.05	69.52±0.45
CD	0.76±0.01	1.18±0.06	2.16±0.18	25.82±2.02	43.84±0.12	62.13±0.45	69.52±0.45
Herding	0.34±0.01	1.7±0.13	4.17±0.26	17.41±0.34	28.06±0.05	48.58±0.49	69.52±0.45
K-Center Greedy	0.76±0.01	1.57±0.09	2.96±0.24	27.36±0.08	44.84±1.03	62.12±0.46	69.52±0.45
Least Confidence	0.29±0.04	1.03±0.25	2.05±0.38	27.05±3.25	44.47±1.42	61.8±0.33	69.52±0.45
Entropy	0.31±0.02	1.01±0.17	2.26±0.3	28.21±2.83	44.68±1.54	61.82±0.31	69.52±0.45
Margin	0.47±0.02	1.99±0.29	4.73±0.64	35.99±1.67	50.29±0.92	63.62±0.15	69.52±0.45
Forgetting	0.76±0.01	4.69±0.17	14.02±0.13	47.64±0.03	55.12±0.13	62.49±0.11	69.52±0.45
GraNd	1.04±0.04	7.02±0.05	18.1±0.22	43.53±0.19	49.92±0.21	57.98±0.17	69.52±0.45
CAL	**1.29±0.09**	7.5±0.26	15.94±1.3	38.32±0.78	46.49±0.29	58.31±0.32	69.52±0.45
Craig	1.13±0.08	5.44±0.52	9.4±1.69	32.3±1.24	38.77±0.56	44.89±3.72	69.52±0.45
GradMatch	0.93±0.04	5.2±0.22	12.28±0.49	40.16±2.28	45.91±1.73	52.69±2.16	69.52±0.45
Glister	0.98±0.06	5.91±0.42	14.87±0.14	44.95±0.28	52.04±1.18	60.26±0.28	69.52±0.45
FL	1.23±0.03	5.78±0.08	12.72±0.21	40.85±1.25	51.05±0.59	63.14±0.03	69.52±0.45
GraphCut	1.21±0.09	7.66±0.43	16.43±0.53	42.23±0.6	50.53±0.42	63.22±0.26	69.52±0.45
RS2 w/ repl	0.17±0.03	16.35±0.56	44.45±0.07	45.4±7.18	64.87±0.10	68.23±0.07	69.52±0.45
RS2 w/ repl (stratified)	0.18±0.02	**33.66±0.13**	**46.96±0.13**	62.32±0.08	64.92±0.10	**68.24±0.08**	69.52±0.45
RS2 w/o repl	0.19±0.02	18.2±0.35	44.42±0.04	**63.2±0.07**	**66.0±0.18**	68.19±0.06	69.52±0.45

static subsets only once before training begins reach just 36% in this setting.

We now focus on additional results to accompany the runtime and time-to-accuracy results presented in the main body of the paper. Specifically, in Table 8, we show the total time needed for subset selection on CIFAR10 across all rounds for RS2 and compare to the total time needed for subset selection for existing data pruning methods which sample a static subset once before learning begins. In Table 9 we show the same measurement for our baseline methods which utilize repeated sampling between each round. Note that the differences presented in these tables are the dominant factor leading to differences in end-to-end runtime between methods: Once a subset has been selected for training at each round, all methods train on the same number of examples, and thus have the same per-round training time (assuming there is no noise). Thus the method with the lowest subset selection overhead will also be the fastest method for end-to-end training.

Table 8 shows that sampling a static random subset once before training leads to the lowest total subset selection time, but that repeated random sampling (RS2) also has low subset selection overhead, i.e., generally less than one second on CIFAR10. The subset selection overhead of RS2 is orders-of-magnitude less than existing methods, even though they sample the subset only once at the beginning of training. For example, most existing methods require over 200 seconds for subset selection because they require pretraining an auxiliary model on the full dataset for a few epochs in order to rank example importance. Some methods, however, require even more time for subset selection; Active Learning based methods can require more than 32,000 seconds to select a subset with $r = 50\%$. Once example importance has been calculated, Table 9 shows that this information can be used to resample the subset for training between each round (our -RS baseline methods, see Section 5.2) with little additional overhead. All such methods, however, still require orders of magnitude more time for subset selection compared to RS2 due to the initial pretraining[1]. On the other hand, recomputing the most important examples between each round (our -RC methods), leads to increased subset selection overhead. The reason for this is that reranking example importance requires computing the model forward pass for all training examples between each round. Thus, such methods generally are unable to significantly reduce the end-to-end runtime compared to simply training on the full dataset each round; Even with a selection ratio of 5%, the fastest -RC method requires more than 3500 seconds for subset selection, yet end-to-end training, each round on the full dataset, requires only 4500 seconds.

Finally, as our primary focus is on reducing time-to-accuracy, we include in Tables 10-14 the time for select baseline methods and RS2 to reach a set of accuracy targets when training with varying pruning ratios on CIFAR10 and ImageNet. For the active learning time-to-accuracy results in these tables, we report the runtime of the smallest selection ratio that reached the given accuracy. This prevents active learning time-to-accuracies from being dominated by large subset selection overheads as the selection ratio increases (e.g., Table 8), when these selection ratios are not strictly needed to reach the

[1]We note that the pretraining overhead of GraNd in Table 8 uses the default hyperparameters from (Guo et al., 2022) in which the results from 10 pretrained auxiliary models are averaged, but for GraNd-RS in Table 9 we use only one model for consistency across all -RS methods.

Table 7: Accuracy achieved by select data pruning methods when training ResNet-18 on CIFAR100 and ImageNet30. Best method bolded; Next best underlined.

Dataset	Select Ratio (r)	10%	20%	30%	40%	50%	60%	70%	80%	90%	100%
CIFAR100	Random	32.0±0.9	53.6±0.6	63.6±0.5	67.2±0.5	71.0±0.3	73.1±0.4	75.2±0.2	76.1±0.3	77.5±0.2	78.7±0.2
	K-Center Greedy	33.9±1.5	56.2±0.9	64.5±0.6	69.8±0.4	72.1±0.5	74.3±0.4	75.8±0.3	77.2±0.2	77.8±0.2	78.7±0.2
	Margin	18.7±2.1	38.2±1.6	58.1±0.8	65.1±0.6	70.1±0.5	73.3±0.3	75.4±0.3	76.9±0.4	78.5±0.2	78.7±0.2
	Forgetting	35.4±1.0	54.7±0.9	64.6±0.7	68.6±0.8	71.5±0.4	73.7±0.5	75.5±0.3	76.1±0.3	76.9±0.3	78.7±0.2
	GraNd	30.8±1.9	49.4±1.0	62.8±0.9	68.1±0.6	70.5±0.3	72.5±0.4	74.5±0.3	76.4±0.2	77.8±0.2	78.7±0.2
	Glister	36.4±1.0	55.5±1.0	63.9±0.8	69.1±0.7	71.2±0.6	73.5±0.4	75.0±0.3	76.9±0.2	77.6±0.2	78.7±0.2
	GraphCut	36.3±1.1	56.0±0.8	65.5±0.6	69.5±0.4	71.1±0.4	73.8±0.4	75.4±0.2	76.4±0.2	78.0±0.2	78.7±0.2
	AL (Conf)	36.1±1.6	55.7±1.0	65.8±0.7	70.6±0.5	73.7±0.4	76.1±0.5	77.1±0.3	78.0±0.2	78.4±0.2	78.7±0.2
	AL (LL)	33.1±1.9	55.3±1.3	64.9±0.8	70.3±0.7	73.1±0.5	75.9±0.5	77.0±0.3	78.2±0.3	78.5±0.2	78.7±0.2
	AL (Margin)	36.0±1.0	57.3±0.5	66.0±0.6	70.4±0.5	73.6±0.5	76.1±0.4	77.2±0.3	78.2±0.3	78.5±0.2	78.7±0.2
	SSP-Easy	32.8±2.0	50.0±1.5	62.5±1.5	67.9±0.3	70.2±0.2	73.4±0.3	75.0±0.7	76.3±0.6	77.4±0.1	78.7±0.2
	SSP-Hard	29.7±1.5	53.3±0.6	63.2±0.5	67.8±0.2	71.3±0.2	72.9±0.2	74.8±0.1	75.9±0.8	77.1±0.2	78.7±0.2
	SP-Easy	33.6±0.9	53.0±2.0	63.0±1.0	67.4±1.0	70.5±0.3	73.3±0.2	74.9±0.2	76.3±0.6	76.9±0.3	78.7±0.2
	SP-Hard	31.2±2.7	53.6±0.4	63.0±0.6	68.0±0.8	71.1±0.3	73.0±0.4	74.6±0.8	75.8±0.9	77.4±0.4	78.7±0.2
	SP-Easy-RS	66.1±1.8	72.7±0.6	74.6±0.5	75.5±0.2	76.3±0.3	76.9±0.4	77.6±0.1	78.0±0.1	78.3±0.3	78.7±0.2
	RS2 w/ repl	68.8±1.5	74.4±0.1	**76.1±0.3**	76.8±0.1	**77.6±0.2**	77.7±0.0	**78.3±0.3**	**78.4±0.2**	**78.7±0.1**	78.7±0.2
	RS2 w/ repl (stratified)	68.6±2.1	74.6±0.7	75.9±0.2	76.7±0.2	77.5±0.1	77.7±0.1	78.1±0.3	78.2±0.2	78.3±0.3	78.7±0.2
	RS2 w/o repl	**73.0±0.3**	**74.9±0.7**	**76.1±0.5**	**77.1±0.1**	77.5±0.4	**78.0±0.1**	**78.3±0.2**	78.3±0.2	78.4±0.3	78.7±0.2
ImageNet30	Random	69.3±0.7	83.7±0.5	86.9±0.4	90.3±0.3	92.2±0.3	93.0±0.2	94.6±0.3	95.2±0.2	95.4±0.2	96.1±0.1
	K-Center Greedy	69.7±0.9	84.1±0.5	88.9±0.4	91.6±0.3	93.4±0.2	94.4±0.3	95.1±0.2	95.3±0.2	95.6±0.2	96.1±0.1
	Margin	56.9±1.1	77.3±0.7	83.7±0.5	90.5±0.4	92.9±0.2	94.4±0.3	95.1±0.2	**95.8±0.2**	**96.0±0.1**	96.1±0.1
	Forgetting	64.1±0.9	85.4±0.7	87.3±0.5	90.9±0.3	93.6±0.4	94.8±0.2	94.9±0.2	95.1±0.2	95.3±0.2	96.1±0.1
	GraNd	69.3±0.9	85.7±0.5	90.0±0.5	92.4±0.4	93.6±0.3	94.7±0.4	95.1±0.2	95.5±0.2	95.7±0.1	96.1±0.1
	Glister	72.4±0.7	82.9±0.5	87.0±0.4	91.2±0.3	92.7±0.3	93.3±0.3	94.2±0.2	95.0±0.2	95.8±0.2	96.1±0.1
	GraphCut	71.9±0.6	83.0±0.3	88.5±0.3	91.2±0.3	92.9±0.2	93.7±0.3	94.4±0.2	95.3±0.2	95.6±0.2	96.1±0.1
	AL (Conf)	70.7±1.1	87.0±0.5	90.3±0.5	93.1±0.4	94.3±0.3	95.1±0.2	95.5±0.4	95.7±0.2	**96.0±0.1**	96.1±0.1
	AL (LL)	68.4±1.5	85.5±0.7	89.3±0.6	93.1±0.5	94.7±0.2	95.3±0.2	95.6±0.3	**95.8±0.2**	**96.0±0.2**	96.1±0.1
	AL (Margin)	71.9±0.9	86.7±0.5	90.1±0.4	93.3±0.4	94.5±0.3	95.1±0.2	95.6±0.3	**95.8±0.2**	**96.0±0.2**	96.1±0.1
	SSP-Easy	71.3±0.5	81.5±2.0	87.4±0.7	90.2±0.3	92.0±0.5	93.1±0.4	94.2±0.2	94.9±0.1	95.3±0.2	96.1±0.1
	SSP-Hard	70.4±1.7	83.0±0.7	87.4±0.3	91.1±0.2	92.9±0.2	93.2±0.7	94.5±0.2	94.9±0.4	95.2±0.2	96.1±0.1
	SP-Easy	70.0±1.5	82.4±0.3	87.1±1.3	89.9±0.6	92.0±0.4	93.4±0.2	94.3±0.3	94.6±0.2	95.4±0.0	96.1±0.1
	SP-Hard	68.0±1.2	81.6±0.3	87.6±0.7	90.8±0.8	92.7±0.6	93.7±0.3	94.3±0.2	94.8±0.4	95.3±0.2	96.1±0.1
	SP-Easy-RS	89.1±0.9	92.3±0.1	93.2±0.5	93.8±0.4	94.5±0.3	95.0±0.3	94.9±0.2	95.4±0.3	95.7±0.2	96.1±0.1
	RS2 w/ repl	91.7±0.6	93.7±0.2	94.2±0.6	**94.9±0.2**	**95.3±0.2**	95.0±0.1	95.4±0.4	95.6±0.2	95.9±0.1	96.1±0.1
	RS2 w/ repl (stratified)	91.7±0.6	93.6±0.3	**94.8±0.4**	**94.9±0.3**	95.2±0.1	**95.4±0.3**	95.5±0.0	95.6±0.3	95.9±0.2	96.1±0.1
	RS2 w/o repl	**92.0±0.4**	**94.0±0.4**	94.6±0.2	94.5±0.3	95.2±0.3	95.3±0.2	**95.7±0.1**	**95.8±0.3**	95.8±0.1	96.1±0.1

desired accuracy. As shown in the main body of the paper, RS2 provides the fastest time-to-accuracy compared to existing methods. Dashes indicate that the given method and pruning ratio failed to reach the target accuracy. We leave a detailed study of these results for future work. In particular, an interesting question is how to decide what pruning ratio r one should use in order to minimize runtime to reach a desired accuracy.

Table 8: Comparison of the total time needed for subset selection for different data pruning methods when training on CIFAR10. Time reported in seconds. The overhead of repeated random sampling is considerably less than existing data pruning methods. For reference, training on the full dataset for 200 epochs takes roughly 4500 seconds. Best method bolded; Next best underlined.

Select Ratio (r)	1%	5%	10%	20%	30%	40%	50%
Random	**0.001±0.0**	**0.001±0.0**	**0.001±0.0**	**0.001±0.0**	**0.001±0.0**	**0.001±0.0**	**0.001±0.0**
CD	237.78±3.08	243.73±6.06	247.01±13.72	244.39±3.58	243.42±2.18	254.46±9.87	254.72±2.28
Herding	238.29±3.84	241.31±2.37	253.0±5.84	258.49±12.35	255.08±0.8	268.91±8.13	263.16±2.84
K-Center Greedy	238.42±2.75	243.16±0.16	243.12±5.1	246.71±5.54	252.07±3.21	260.44±5.2	259.34±1.68
Least Confidence	238.61±2.6	238.08±2.59	241.96±5.89	239.92±3.72	237.07±1.64	239.47±6.53	240.01±5.08
Entropy	239.44±0.91	242.48±1.41	239.57±5.57	242.79±7.49	235.59±1.44	240.67±2.19	239.68±2.0
Margin	241.71±2.58	245.28±5.89	246.17±4.65	240.83±1.5	243.12±1.24	241.4±4.05	243.45±1.32
Forgetting	235.34±1.82	238.09±6.87	237.93±5.57	235.44±1.96	234.9±4.17	235.97±7.32	234.78±1.57
GraNd	2372.95±22.89	2406.41±79.95	2384.34±13.3	2377.09±16.19	2396.31±27.83	2375.14±17.84	2389.62±34.32
CAL	559.68±1.43	562.32±22.51	558.97±1.96	557.83±10.9	568.95±10.64	559.37±5.04	553.13±9.83
Craig	296.27±2.94	322.16±3.83	362.8±10.12	438.21±13.49	506.38±10.17	572.06±2.95	642.26±12.05
Glister	244.66±3.99	242.02±4.24	247.44±3.41	248.03±8.07	254.79±1.62	259.26±5.81	259.58±5.36
FL	330.79±20.94	587.43±16.07	764.18±86.51	1261.9±165.55	1863.98±241.04	2151.46±435.54	2722.44±145.36
GraphCut	325.66±9.37	551.81±46.75	728.66±45.93	1251.72±187.75	1601.92±202.89	2335.62±495.53	2672.69±643.3
AL (Conf)	408.3±8.4	908.1±9.8	2152.8±23.7	6694.8±80.6	13358.8±184.5	22120.2±329.5	32940.6±418.7
AL (LL)	398.5±5.4	879.1±9.8	2087.2±21.0	6592.5±43.9	13206.8±172.9	21933.8±362.6	32763.1±596.6
AL (Margin)	396.3±19.9	875.3±36.2	2107.2±73.6	6634.9±149.1	13298.5±241.1	22062.8±275.7	32871.6±425.9
SSP-Easy	265.67±5.87	269.89±8.48	268.44±8.51	263.84±6.49	264.85±5.58	268.21±5.82	269.39±4.78
SSP-Hard	285.91±9.25	288.47±8.07	290.3±26.43	284.52±27.16	293.41±21.92	287.28±25.74	271.59±6.09
SP-Easy	229.04±2.46	231.09±3.94	231.47±4.36	233.61±6.34	233.86±3.38	231.58±5.65	233.6±4.32
SP-Hard	227.68±1.65	234.39±1.2	230.85±3.65	227.67±2.23	231.66±2.64	230.97±3.1	233.12±5.94
RS2 w/ repl	<u>0.16±0.01</u>	<u>0.16±0.01</u>	<u>0.16±0.01</u>	<u>0.16±0.01</u>	<u>0.16±0.01</u>	<u>0.16±0.01</u>	<u>0.16±0.01</u>
RS2 w/ repl (stratified)	0.68±0.02	0.72±0.03	0.75±0.01	0.84±0.03	0.93±0.05	1.0±0.03	1.09±0.03
RS2 w/o repl	0.09±0.01	0.1±0.01	0.11±0.01	0.12±0.01	0.14±0.01	0.15±0.01	0.19±0.01

Table 9: Comparison of the total time (in seconds) needed for subset selection for our dynamic data pruning methods when training on CIFAR10. The training subset is update for all methods after each round, either by resampling from a static example importance distribution (RS, left) or by recomputing example importance based on model updates (RC, right). For reference, training on the full dataset for 200 epochs takes roughly 4500 seconds. Best method bolded; Next best underlined.

Selection Ratio (r)	5%	10%	30%
CD-RS	-	-	-
Herding-RS	-	-	-
K-Center Greedy-RS	-	-	-
Least Confidence-RS	238.9±2.66	244.12±3.5	243.75±9.7
Entropy-RS	241.26±2.63	240.41±1.33	247.27±3.19
Margin-RS	243.46±3.29	239.53±4.26	239.27±3.36
Forgetting-RS	<u>236.3±5.61</u>	<u>239.38±2.36</u>	<u>236.24±4.24</u>
GraNd-RS	397.92±0.56	409.93±9.32	406.89±4.74
CAL-RS	555.75±20.87	549.93±10.61	547.82±3.33
Craig-RS	1025.14±70.46	987.05±16.13	1021.92±13.77
Glister-RS	-	-	-
SP-Easy-RS	326.76 ± 63.77	371.23 ± 63.71	497.39 ± 8.69
RS2 w/ repl (stratified)	0.72 ± 0.03	0.75 ± 0.01	0.93 ± 0.05
RS2 w/o repl	**0.1±0.01**	**0.11±0.01**	**0.14±0.01**

Selection Ratio (r)	5%	10%	30%
CD-RC	<u>3581.05±61.15</u>	3860.4±31.36	4860.18±55.95
Herding-RC	3851.82±37.15	4332.73±31.25	6578.17±9.45
K-Center Greedy-RC	3854.89±39.84	4384.02±38.72	6282.79±35.03
Least Confidence-RC	3698.25±47.31	<u>3674.73±37.97</u>	<u>3630.66±30.48</u>
Entropy-RC	3651.39±15.2	3677.18±32.94	3690.08±27.57
Margin-RC	3715.31±75.59	3686.48±24.21	3760.33±91.99
Forgetting-RC	3756.12±25.54	3732.81±33.9	3723.22±39.52
GraNd-RC	38035.57±1212.62	37390.35±939.82	29134.04±16123.62
CAL-RC	69994.0±200.65	66947.73±2645.88	67086.71±1213.57
Craig-RC	20517.31±955.04	27497.62±359.82	55305.63±988.66
Glister-RC	4358.65±56.65	4966.57±20.48	6393.25±33.59
SP-Easy-RC	-	-	-
RS2 w/ repl (stratified)	0.72 ± 0.03	0.75 ± 0.01	0.93 ± 0.05
RS2 w/o repl	**0.1±0.01**	**0.11±0.01**	**0.14±0.01**

Table 10: The total time required for RS2 and baseline data pruning methods to reach a target accuracy (time-to-accuracy) when training with varying pruning ratios on CIFAR10. Time is reported in seconds. Part 1/3. The best method(s) is bolded.

Target	Select Ratio (r)	1%	5%	10%	20%	30%	40%	50%	60%	70%	80%	90%
30% acc	Random	73	**16**	28	**23**	**15**	**20**	**13**	**14**	**16**	**18**	**20**
	CD	-	332	372	289	297	284	290	283	286	294	283
	Herding	-	295	296	275	283	279	273	278	281	285	291
	K-Center Greedy	353	284	304	273	267	280	283	281	283	290	296
	Least Confidence	-	-	393	330	299	278	275	265	259	262	264
	Entropy	-	484	398	346	289	270	274	267	256	259	262
	Margin	-	324	381	297	297	271	279	264	272	259	263
	Forgetting	302	263	299	264	258	264	258	249	257	252	253
	GraNd	-	2485	2461	2422	2428	2404	2425	2397	2376	2471	2387
	CAL	-	596	597	574	385	579	565	605	605	591	595
	Craig	365	342	395	461	521	583	668	740	816	909	952
	Glister	-	280	274	264	270	278	283	278	280	291	293
	FL	377	605	803	1279	1878	2179	2734	3239	3671	4696	4513
	GraphCut	371	567	771	1268	1617	2355	2684	3462	3771	4427	4458
	AL (Conf)	395	395	395	395	395	395	395	395	395	395	395
	AL (LL)	386	386	386	386	386	386	386	386	386	386	386
	AL (Margin)	383	383	383	383	383	383	383	383	383	383	383
	SSP-Easy	320	295	300	280	288	287	281	282	282	287	289
	SSP-Hard	403	325	330	307	309	308	283	283	286	293	289
	SP-Easy	295	246	258	249	246	254	240	243	249	243	253
	SP-Hard	315	260	262	250	247	250	257	250	251	248	252
	SP-Easy-RS	284	249	256	262	249	250	257	249	250	249	252
	RS2 w/ repl	67	**19**	36	21	**15**	**19**	**12**	**14**	**16**	**18**	**20**
	RS2 w/ repl (stratified)	**59**	**20**	43	27	**15**	**19**	**12**	**14**	**15**	**18**	**20**
	RS2 w/o repl	83	**17**	**14**	**11**	**15**	**19**	**11**	**14**	**16**	**18**	**20**
50% acc	Random	-	78	109	65	55	69	49	56	48	**54**	61
	CD	-	-	617	354	366	384	361	325	318	349	304
	Herding	-	-	564	399	345	319	322	320	314	323	311
	K-Center Greedy	-	390	397	322	314	309	318	323	331	327	317
	Least Confidence	-	-	-	438	383	357	347	321	325	335	306
	Entropy	-	-	-	513	412	339	345	324	321	314	303
	Margin	-	-	755	439	407	359	351	305	305	314	304
	Forgetting	-	-	455	366	350	333	306	305	306	306	295
	GraNd	-	-	2811	2550	2531	2484	2498	2453	2408	2509	2428
	CAL	-	881	764	652	633	630	612	648	638	628	635
	Craig	-	458	523	537	568	633	704	782	885	946	993
	Glister	-	393	372	313	308	319	307	334	312	328	313
	FL	-	695	909	1341	1917	2219	2771	3267	3704	4733	4535
	GraphCut	-	623	876	1321	1664	2395	2720	3506	3805	4463	4478
	AL (Conf)	-	895	895	895	895	895	895	895	895	895	895
	AL (LL)	-	867	867	867	867	867	867	867	867	867	867
	AL (Margin)	-	862	862	862	862	862	862	862	862	862	862
	SSP-Easy	-	375	394	336	333	336	316	323	314	324	329
	SSP-Hard	-	432	433	365	357	358	332	326	335	330	329
	SP-Easy	-	340	362	306	301	284	287	271	282	261	293
	SP-Hard	-	277	354	312	301	290	306	294	284	285	291
	SP-Easy-RS	-	308	355	335	289	298	304	290	282	267	273
	RS2 w/ repl	279	77	137	66	61	**48**	47	56	48	**55**	61
	RS2 w/ repl (stratified)	**250**	87	123	83	69	60	72	57	64	**54**	**40**
	RS2 w/o repl	-	**64**	**44**	**46**	**46**	58	**35**	**41**	**32**	**53**	60

Table 11: The total time required for RS2 and baseline data pruning methods to reach a target accuracy (time-to-accuracy) when training with varying pruning ratios on CIFAR10. Time is reported in seconds. Part 2/3. The best method(s) is bolded.

Target	Select Ratio (r)	1%	5%	10%	20%	30%	40%	50%	60%	70%	80%	90%
70% acc	Random	-	-	364	216	184	139	136	139	130	126	143
	CD	-	-	-	584	504	473	456	396	382	421	406
	Herding	-	-	-	926	760	456	406	418	395	415	393
	K-Center Greedy	-	-	552	420	384	397	414	380	412	493	379
	Least Confidence	-	-	-	911	514	455	453	420	374	372	369
	Entropy	-	-	-	954	565	457	464	423	371	387	385
	Margin	-	-	-	705	564	479	473	387	402	387	366
	Forgetting	-	-	-	549	473	430	366	376	374	360	356
	GraNd	-	-	-	2727	2689	2573	2583	2523	2489	2584	2489
	CAL	-	-	-	1025	801	763	720	748	719	720	695
	Craig	-	-	775	664	693	724	803	854	966	1020	1075
	Glister	-	-	601	429	409	418	390	406	393	383	396
	FL	-	-	1144	1467	2009	2299	2855	3326	3785	4807	4597
	GraphCut	-	-	1136	1465	1734	2484	2804	3578	3889	4536	4538
	AL (Conf)	-	-	2884	2884	2884	2884	2884	2884	2884	2884	2884
	AL (LL)	-	-	2804	2804	2804	2804	2804	2804	2804	2804	2804
	AL (Margin)	-	-	2833	2833	2833	2833	2833	2833	2833	2833	2833
	SSP-Easy	-	-	716	445	440	404	412	407	410	399	390
	SSP-Hard	-	-	689	532	461	438	392	411	416	404	411
	SP-Easy	-	-	705	431	409	403	370	355	363	332	373
	SP-Hard	-	-	586	428	379	398	402	380	365	357	372
	SP-Easy-RS	-	440	508	415	383	374	377	358	378	339	354
	RS2 w/ repl	-	**218**	271	205	162	147	130	154	**112**	128	142
	RS2 w/ repl (stratified)	-	**213**	260	179	155	151	144	**126**	145	126	**121**
	RS2 w/o repl	-	**201**	**168**	**128**	**116**	**127**	**105**	**125**	**112**	**107**	**122**
80% acc	Random	-	-	-	553	470	395	303	**266**	277	**199**	306
	CD	-	-	-	917	713	654	601	494	495	567	508
	Herding	-	-	-	-	-	1522	1222	909	686	598	536
	K-Center Greedy	-	-	-	692	695	635	606	535	557	511	563
	Least Confidence	-	-	-	-	738	622	621	587	537	518	534
	Entropy	-	-	-	-	912	675	584	521	516	498	529
	Margin	-	-	-	-	975	678	606	538	548	496	509
	Forgetting	-	-	-	719	641	616	511	518	541	451	538
	GraNd	-	-	-	2984	2831	2671	2681	2636	2585	2716	2650
	CAL	-	-	-	-	1378	1132	995	978	968	921	816
	Craig	-	-	-	1057	1063	1075	986	1111	1116	1242	1218
	Glister	-	-	-	788	650	687	614	604	586	494	559
	FL	-	-	-	1765	2331	2525	3122	3528	3997	4936	4742
	GraphCut	-	-	-	1779	2068	2681	3049	3782	4106	4735	4697
	AL (Conf)	-	-	2884	2884	2884	2884	2884	2884	2884	2884	2884
	AL (LL)	-	-	2804	2804	2804	2804	2804	2804	2804	2804	2804
	AL (Margin)	-	-	2833	2833	2833	2833	2833	2833	2833	2833	2833
	SSP-Easy	-	-	-	814	712	639	638	629	553	583	592
	SSP-Hard	-	-	-	840	786	739	584	625	626	570	573
	SP-Easy	-	-	-	839	702	699	617	466	461	493	595
	SP-Hard	-	-	-	766	673	605	558	578	496	503	514
	SP-Easy-RS	-	564	634	637	585	501	590	567	490	538	516
	RS2 w/ repl	-	**331**	383	334	308	343	274	293	337	312	324
	RS2 w/ repl (stratified)	-	**331**	339	320	317	341	289	295	275	272	303
	RS2 w/o repl	-	**333**	**278**	**257**	**278**	**264**	**212**	**264**	**241**	270	**264**

Table 12: The total time required for RS2 and baseline data pruning methods to reach a target accuracy (time-to-accuracy) when training with varying pruning ratios on CIFAR10. Time is reported in seconds. Part 3/3. The best method(s) is bolded.

Target	Select Ratio (r)	1%	5%	10%	20%	30%	40%	50%	60%	70%	80%	90%
90% acc	Random	-	-	-	-	1473	1462	1722	1906	2037	2149	2403
	CD	-	-	-	-	1327	1615	1806	1917	2002	2181	2461
	Herding	-	-	-	-	-	-	2736	2801	2810	2885	2839
	K-Center Greedy	-	-	-	-	1412	1662	1913	2093	2310	2433	2433
	Least Confidence	-	-	-	-	1446	1546	1746	1940	2080	2268	2423
	Entropy	-	-	-	-	-	1542	1783	1892	2024	2255	2468
	Margin	-	-	-	-	-	1554	1749	1877	2020	2151	2498
	Forgetting	-	-	-	-	1359	1569	1699	1969	2228	2334	2562
	GraNd	-	-	-	-	3530	3645	3845	3889	4042	4465	4531
	CAL	-	-	-	-	-	2201	2292	2459	2658	2692	3042
	Craig	-	-	-	-	1798	2024	2381	2613	2982	3134	3030
	Glister	-	-	-	-	1718	1734	1885	2222	2368	2485	2639
	FL	-	-	-	-	3203	3591	4454	5229	5715	6903	6707
	GraphCut	-	-	-	-	2846	3782	4428	5387	5860	6459	6782
	AL (Conf)	-	-	-	7845	7845	7845	7845	7845	7845	7845	7845
	AL (LL)	-	-	-	7740	7740	7740	7740	7740	7740	7740	7740
	AL (Margin)	-	-	-	7787	7787	7787	7787	7787	7787	7787	7787
	SSP-Easy	-	-	-	-	1534	1719	1932	2152	2329	2582	2546
	SSP-Hard	-	-	-	-	1740	1760	1961	2155	2273	2452	2499
	SP-Easy	-	-	-	-	-	1699	1936	2126	2324	2323	2647
	SP-Hard	-	-	-	-	-	1712	1906	2157	2206	2407	2650
	SP-Easy-RS	-	-	-	1080	1284	1505	1721	1962	2173	2365	2619
	RS2 w/ repl	-	-	-	777	1028	**1220**	1435	1645	1893	**1979**	2378
	RS2 w/repl (stratified)	-	-	-	785	995	1267	1483	**1577**	**1786**	2099	**2127**
	RS2 w/o repl	-	-	**566**	**723**	**953**	**1211**	**1291**	1637	1866	2106	2357
95% acc	Random	-	-	-	-	-	-	-	-	-	-	3582
	CD	-	-	-	-	-	-	-	-	3124	3416	3784
	Herding	-	-	-	-	-	-	-	-	-	-	3815
	K-Center Greedy	-	-	-	-	-	-	-	-	-	-	3952
	Least Confidence	-	-	-	-	-	-	-	-	3084	3432	3838
	Entropy	-	-	-	-	-	-	-	2900	3171	3464	3822
	Margin	-	-	-	-	-	-	-	-	3057	3522	3797
	Forgetting	-	-	-	-	-	-	-	-	-	-	3835
	GraNd	-	-	-	-	-	-	-	-	5133	5721	5956
	CAL	-	-	-	-	-	-	-	-	-	-	4153
	Craig	-	-	-	-	-	-	-	-	-	-	-
	Glister	-	-	-	-	-	-	-	-	-	-	4012
	FL	-	-	-	-	-	-	-	-	-	-	8221
	GraphCut	-	-	-	-	-	-	-	-	-	-	8028
	AL (Conf)	-	-	-	-	-	-	-	48708	48708	48708	48708
	AL (LL)	-	-	-	-	-	-	-	48549	48549	48549	48549
	AL (Margin)	-	-	-	-	-	-	-	48326	48326	48326	48326
	SSP-Easy	-	-	-	-	-	-	-	-	-	-	-
	SSP-Hard	-	-	-	-	-	-	-	-	-	-	3908
	SP-Easy	-	-	-	-	-	-	-	-	-	-	4214
	SP-Hard	-	-	-	-	-	-	-	-	-	-	3922
	SP-Easy-RS	-	-	-	-	-	-	-	-	3180	3505	3810
	RS2 w/ repl	-	-	-	-	-	-	2296	**2498**	**2856**	3245	3696
	RS2 w/repl (stratified)	-	-	-	-	-	-	-	2585	3003	3300	**3501**
	RS2 w/o repl	-	-	-	-	-	-	**2153**	2633	2943	**3147**	3569

Table 13: The total time required for RS2 and select baseline data pruning methods to reach a target accuracy (time-to-accuracy) when training with varying pruning ratios on ImageNet. Time is reported in seconds. Part 1/2. The best method(s) is bolded.

Target	Select Ratio (r)	1%	5%	10%
5% acc	Random	919	**289**	**231**
	Herding	22222	27794	24243
	Least Confidence	-	15292	19362
	Entropy	-	19535	19285
	Margin	19494	14121	15785
	Forgetting	19081	18394	15978
	GraNd	146059	143640	147931
	FL	67907	67789	220647
	GraphCut	66336	224755	303318
	RS2 w/ repl	542	347	**231**
	RS2 w/ repl (stratified)	**403**	**291**	350
	RS2 w/o repl	530	347	347
10% acc	Random	2003	**462**	579
	Herding	-	29468	24822
	Least Confidence	-	16043	20056
	Entropy	-	20517	19864
	Margin	-	14698	16364
	Forgetting	19799	18625	16094
	GraNd	14743	143755	148047
	FL	69144	220878	308052
	GraphCut	66831	224928	303434
	RS2 w/ repl	931	635	**463**
	RS2 w/ repl (stratified)	**686**	638	581
	RS2 w/o repl	907	635	**463**
20% acc	Random	-	1906	**1157**
	Herding	-	-	36974
	Least Confidence	-	22684	23065
	Entropy	-	27158	22757
	Margin	-	19029	17984
	Forgetting	-	20877	16557
	GraNd	-	146123	148741
	FL	-	221802	308630
	GraphCut	-	225794	304012
	RS2 w/ repl	1355	1502	1273
	RS2 w/ repl (stratified)	**1145**	**1388**	**1160**
	RS2 w/o repl	1308	**1386**	**1157**
30% acc	Random	-	7219	4282
	Herding	-	-	-
	Least Confidence	-	-	32555
	Entropy	-	-	32131
	Margin	-	43750	25159
	Forgetting	-	25959	18293
	GraNd	-	151840	158347
	FL	-	227519	313954
	GraphCut	-	307600	307600
	RS2 w/ repl	1626	3927	4514
	RS2 w/ repl (stratified)	**1546**	**3583**	3937
	RS2 w/o repl	1673	4100	**3166**

Table 14: The total time required for RS2 and select baseline data pruning methods to reach a target accuracy (time-to-accuracy) when training with varying pruning ratios on ImageNet. Time is reported in seconds. Part 2/2. The best method(s) is bolded.

Target	Select Ratio (r)	1%	5%	10%
40% acc	Random	-	-	14814
	Herding	-	-	-
	Least Confidence	-	-	-
	Entropy	-	-	-
	Margin	-	-	32682
	Forgetting	-	-	28824
	GraNd	-	-	166680
	FL	-	-	322518
	GraphCut	-	234399	317553
	RS2 w/ repl	2015	6815	**11689**
	RS2 w/ repl (stratified)	**1864**	**6586**	11923
	RS2 w/o repl	2015	6699	12152
50% acc	Random	-	-	-
	Herding	-	-	-
	Least Confidence	-	-	-
	Entropy	-	-	-
	Margin	-	-	-
	Forgetting	-	-	35305
	GraNd	-	-	-
	FL	-	-	-
	GraphCut	-	-	-
	RS2 w/ repl	-	8605	16550
	RS2 w/ repl (stratified)	-	**8492**	16552
	RS2 w/o repl	-	8605	**16434**
60% acc	Random	-	-	-
	Herding	-	-	-
	Least Confidence	-	-	-
	Entropy	-	-	-
	Margin	-	-	-
	Forgetting	-	-	-
	GraNd	-	-	-
	FL	-	-	-
	GraphCut	-	-	-
	RS2 w/ repl	-	10337	20021
	RS2 w/ repl (stratified)	-	**10282**	20024
	RS2 w/o repl	-	**10280**	**19790**
65% acc	Random	-	-	-
	Herding	-	-	-
	Least Confidence	-	-	-
	Entropy	-	-	-
	Margin	-	-	-
	Forgetting	-	-	-
	GraNd	-	-	-
	FL	-	-	-
	GraphCut	-	-	-
	RS2 w/ repl	-	-	22105
	RS2 w/ repl (stratified)	-	-	22107
	RS2 w/o repl	-	-	**21873**

D. Additional RS2 Pseudocode

In this section, we include additional RS2 pseudocode algorithms to accompany Algorithm 1 presented in the main body of the paper and to present additional details useful for the RS2 theoretical analysis.

In Algorithm 2 we describe RS2 without replacement when training with accelerated mini batch SGD (Ghadimi & Lan, 2016; Nesterov, 1983). Nesterov's accelerated gradient introduces three different sets of parameters that are updated at each iteration t. We denote them as w^t, w^t_{ag}, and w^t_{md}. Furthermore, the algorithm introduces learning rate parameters α_t, β_t, and λ_t. In later sections, we specialize the learning rate parameters for obtaining a convergence rate bound. Finally, $g(w, \xi_t; m)$ at step t represents the gradient estimate on a batch of data m that is used for updating the model. ξ_t are random vectors whose distributions are supported on $\Xi_t \in \mathbb{R}^d$.

Algorithm 2 RS2 w/o Replacement With Accelerated Mini batch SGD

Require: Dataset $S = \{x_i, y_i\}_{i=1}^N$, selection ratio $r \in (0, 1]$, batch size b, initial model w^0, X rounds, learning rate parameters $\{\alpha_t\}$ s.t. $\alpha_1 = 1, \alpha_t \in (0, 1), \forall t \geq 2$, $\{\beta_t > 0\}$, $\{\lambda_t > 0\}$, gradient estimate function for batch m and parameters w with noise ξ: $g(w, \xi; m)$

$T \leftarrow \lceil N/b \rceil$
$t \leftarrow 1$
$w^0_{ag} = w^0$
for round $j = 1$ to X **do**
  if $t\%T == 0$ **then**
    $shuffle(S)$ {Shuffle after full dataset has been seen}
  $S' \leftarrow S[(j-1) \cdot rN : j \cdot rN]$ {Select the subset across rounds without replacement}
  for $k = 1$ to $r \cdot T$ **do**
    batch $m \leftarrow S'[(k-1) \cdot b : k \cdot b]$
    $w^t_{md} \leftarrow (1 - \alpha_t) w^{t-1}_{ag} + \alpha_t w^{t-1}$
    $w^t \leftarrow w^{t-1} - \lambda_t g(w^t_{md}, \xi_t; m)$
    $w^t_{ag} \leftarrow w^t_{md} - \beta_t g(w^t_{md}, \xi_t; m)$
    } {$train\_on\_batch$ for Nesterov mini batch SGD}
    $t \leftarrow t + 1$
return w^t_{md}

In Algorithm 3, we also show RS2 without replacement, but using standard mini batch SGD. We also write this algorithm using a different perspective: instead of iterating over rounds, selecting the training subset for each round, and then iterating over batches in the selected subset, RS2 without replacement can be equivalently implemented by iterating directly over batches from the full dataset, as long as these batches are correctly selected and the full dataset is shuffled as necessary. This perspective can be more useful for understanding the generalization error of RS2 without replacement as it more closely matches the common algorithms in related works analyzing SGD (Ghadimi & Lan, 2016; Nikolakakis et al., 2023).

Algorithm 3 RS2 w/o Replacement With Mini batch SGD; Single For Loop Perspective

Require: Dataset $S = \{x_i, y_i\}_{i=1}^N$, selection ratio $r \in (0, 1]$, batch size b, initial model w^0, X rounds, learning rate η_t

$T \leftarrow \lceil N/b \rceil$
for iterate $t = 1$ to $r \cdot T \cdot X$ **do**
  if $t\%T == 0$ **then**
    $shuffle(S)$ {Shuffle after full dataset has been seen}
  batch $m \leftarrow S[(t-1)\%T \cdot b : t\%T \cdot b]$
  $w^t \leftarrow w^{t-1} - \frac{\eta_t}{b} \sum_{(x,y) \in m} \nabla f(w^{t-1}; x, y)$ {$train\_on\_batch$ for mini batch SGD}
return w^t

E. RS2 Convergence Rate

Performance of accelerated mini batch SGD has been well studied for convex functions (Lan, 2012; Dekel et al., 2012; Cotter et al., 2011). It has been shown that mini batch SGD using batch of size b, after X rounds with T batches per round

returns a solution w satisfying

$$\mathbb{E}[l(w) - l(w^*)] \leq \mathcal{O}\left(\frac{L||w^0 - w^*||^2}{T^2X^2} + \frac{\sigma||w^0 - w^*||}{\sqrt{bTX}}\right). \tag{4}$$

Furthermore, (Ghadimi & Lan, 2016) have analyzed the convergence rate of mini batch SGD for nonconvex β-smooth functions. After TX mini batch steps of size b the algorithm guarantees a solution w such that

$$\mathbb{E}||\nabla l(w)||^2 \leq \mathcal{O}\left(\frac{\beta(l(w^0) - l(w^*))}{TX} + \frac{\sigma\sqrt{\beta(l(w^0) - l(w^*))}}{\sqrt{bTX}}\right). \tag{5}$$

We provide convergence analysis for accelerated mini batch SGD using RS2 without replacement as shown in Algorithm 2 following the analysis of (Ghadimi & Lan, 2016).

Corollary E.1. *Suppose the loss $l(w)$ is nonconvex, has β-Lipschitz continuous gradients, and is bounded below. Let $g(w, \xi_t)$ at step t represent the gradient estimate used when updating the model as in Algorithm 2 in the Appendix. Assume the gradient estimate satisfies $\mathbb{E}\left[||g(w, \xi_t) - \nabla l(w)||^2\right] \leq \sigma^2$, and $\mathbb{E}[g(w, \xi_t)] = \nabla l(w)$, where ξ_t are random vectors whose distributions are supported on $\Xi_t \in \mathbb{R}^d$. With the previous assumptions, using a selection ratio $r \in (0, 1]$ and mini batch of size b, RS2 produces an iterate w after X rounds, with rT batches per round, such that:*

$$\mathbb{E}\left[||\nabla l(w)||^2\right] \leq \mathcal{O}\left(\frac{\beta(l(w^0) - l(w^*))}{r \cdot T \cdot X} + \frac{\sigma\sqrt{\beta(l(w^0) - l(w^*))}}{\sqrt{b \cdot r \cdot T \cdot X}}\right). \tag{6}$$

Furthermore, assuming that $l(w)$ is convex it holds that

$$\mathbb{E}[l(w) - l(w^*)] \leq \mathcal{O}\left(\frac{\beta||w^0 - w^*||^2}{r^2 \cdot T^2 \cdot X^2} + \frac{\sigma||w^0 - w^*||}{\sqrt{b \cdot r \cdot T \cdot X}}\right). \tag{7}$$

Proof. Each round we use Nesterov's accelerated method to update the gradient:

$$w_{md}^t \leftarrow (1 - \alpha_t)w_{ag}^{t-1} + \alpha_t w^{t-1} \tag{8}$$

$$w^t \leftarrow w^{t-1} - \lambda_t g(w_{md}^t, \xi_t; m) \tag{9}$$

$$w_{ag}^t \leftarrow w_{md}^t - \beta_t g(w_{md}^t, \xi_t; m) \tag{10}$$

where $g(w_{md}^t, \xi_t)$ represents the gradient on a batch of data m. We assume that the following holds:

$$\mathbb{E}g(w, \xi_t) = \nabla l(w) \tag{11}$$

$$\mathbb{E}||g(w, \xi_t) - \nabla l(w)||^2 = \sigma^2, \tag{12}$$

where ξ_t are random vectors whose distributions are supported on $\Xi_t \in \mathbb{R}^d$; These are the source of randomness when estimating the full data gradient.

We repeat the procedure for X rounds. When using full data each round we have T batches, resulting in total TX gradient updates. If we perform RS2 w/o replacement. each round we will contain rT updates per round, resulting in a total of rTX iterations. Assume a relaxation for the learning rate parameters. For this part of the proof assume they are chosen $\{\alpha_t\}$ s.t. $\alpha_1 = 1, \alpha_t \in (0, 1), \forall t \geq 2$, $\{\beta_t > 0\}$, $\{\lambda_t > 0\}$, such that the following holds:

$$\Gamma^t = \begin{cases} 1 & t = 1 \\ (1 - \alpha_t)\Gamma^{t-1} & t \geq 2 \end{cases} \tag{13}$$

$$C^t := 1 - \beta\lambda_t - \frac{\beta(\lambda_t - \beta_t)^2}{2\alpha_t\Gamma^t\lambda_t}\left(\sum_{\tau=t}^{rTX}\Gamma^\tau\right) > 0 \tag{14}$$

$$p_t = \frac{\lambda_t C^t}{\sum_{t=1}^{rTX}\lambda_t C^t},\ t = 1, ..., rTX. \tag{15}$$

Furthermore, let R represent an index chosen randomly in all the iterate updates from 1 to rTX, chosen such that $Prob\{R = t\} = p_t$.

First we want to show the following holds:

$$\mathbb{E}||\nabla l(w_{md}^R)||^2 \leq \frac{1}{\sum_{t=1}^{rTX} \lambda_t C^t} \left[l(w^0) - l(w^*) + \frac{\beta\sigma^2}{2} \sum_{t=1}^{rTX} \lambda_t^2 \left(1 + \frac{(\lambda_t - \beta_t)^2}{\alpha_t \Gamma^t \lambda_t^2} \sum_{\tau=t}^{rTX} \Gamma^\tau \right) \right]. \tag{16}$$

Let us define, for ease of writing, the following: $\delta_t := g(w_{md}^t, \xi_t) - \nabla l(w_{md}^t)$ and $\Delta^t := \nabla l(w^{t-1}) - \nabla l(w_{md}^t)$. Since $l(w)$ is bounded from below and a differentiable nonconvex β-smooth function it holds that (see (Nesterov, 2003)):

$$|l(y) - l(x) - \langle \nabla l(x), y - x \rangle| \leq \frac{\beta}{2}||y - x||^2 \quad \forall x, y \in \mathbb{R}^n. \tag{17}$$

We start from the assumption that the loss function l is β-smooth:

$$l(w^t) \leq l(w^{t-1}) + \langle \nabla l(w^{t-1}), w^t - w^{t-1} \rangle + \frac{\beta}{2}||w^t - w^{t-1}||. \tag{18}$$

Then, using the update step Equation (9) and the definitions of δ_t, Δ^t:

$$\begin{aligned} l(w^t) &\leq l(w^{t-1}) + \langle \Delta^t + \nabla l(w_{md}^t), -\lambda_t [\nabla l(w_{md}^t) + \delta^t] \rangle + \frac{\beta\lambda_t^2}{2}||\nabla l(w_{md}^t) + \delta^t||^2 \\ &= l(w^{t-1}) + \langle \Delta^t + \nabla l(w_{md}^t), -\lambda_t \nabla l(w_{md}^t) \rangle - \lambda_t \langle \nabla l(w^{t-1}), \delta^t \rangle + \frac{\beta\lambda_t^2}{2}||\nabla l(w_{md}^t) + \delta^t||^2. \end{aligned} \tag{19}$$

Now using the inequality Equation (17) we get:

$$\begin{aligned} l(w^t) \leq l(w^{t-1}) &- \lambda_t \left(1 - \frac{\beta\delta_t}{2} \right) ||\nabla l(w_{md}^t)||^2 + \lambda_t ||\Delta^t|| ||\nabla l(w_{md}^t)|| + \frac{\beta\lambda_t^2}{2}||\delta^t||^2 \\ &- \lambda_t \langle \nabla l(w^{t-1}) - \beta\lambda_t \nabla l(w_{md}^t), \delta^t \rangle. \end{aligned} \tag{20}$$

Since l is β-smooth and by the update rule Equation (8) we have:

$$||\Delta^t|| = ||\nabla l(w^{t-1}) - \nabla l(w_{md}^t)|| \leq \beta ||w^{t-1} - w_{md}^t|| = \beta(1 - \alpha_t)||w_{ag}^t - w^{t-1}||. \tag{21}$$

Continuing from Equation (19) and inserting Equation (21):

$$\begin{aligned} l(w^t) \leq l(w^{t-1}) &- \lambda_t \left(1 - \frac{\beta\delta_t}{2} \right) ||\nabla l(w_{md}^t)||^2 + \lambda_t \beta(1 - \alpha_t)||w_{ag}^t - w^{t-1}|| ||\nabla l(w_{md}^t)|| \\ &+ \frac{\beta\lambda_t^2}{2}||\delta^t||^2 - \lambda_t \langle \nabla l(w^{t-1}) - \beta\lambda_t \nabla l(w_{md}^t), \delta^t \rangle. \end{aligned} \tag{22}$$

Using the general fact that $xy \leq \frac{(x^2+y^2)}{2}$ holds, we bound the previous inequality:

$$\begin{aligned} l(w^t) \leq l(w^{t-1}) &- \lambda_t (1 - \beta\lambda_t) ||\nabla l(w_{md}^t)||^2 + \frac{\beta(1 - \alpha_t)^2}{2}||w_{ag}^{t-1} - w^{t-1}||^2 + \frac{\beta\lambda_t^2}{2}||\delta^t||^2 \\ &- \lambda_t \langle \nabla l(w^{t-1}) - \beta\lambda_t \nabla l(w_{md}^t), \delta^t \rangle. \end{aligned} \tag{23}$$

Now we take a small digression from the main flow of the proof. We want to show that the following inequality holds:

$$\begin{aligned} ||w_{ag}^{t-1} - w^{t-1}||^2 &\leq \Gamma^{t-1} \sum_{\tau=1}^{t-1} \frac{(\lambda_\tau - \beta_\tau)^2}{\Gamma^\tau \alpha_\tau} ||\nabla l(w_{md}^\tau) + \delta^t||^2 \\ &= \Gamma^{t-1} \sum_{\tau=1}^{t-1} \frac{(\lambda_\tau - \beta_\tau)^2}{\Gamma^\tau \alpha_\tau} \left[||\nabla l(w_{md}^\tau)||^2 + 2\langle \nabla l(w_{md}^\tau), \delta^\tau \rangle + ||\delta^\tau||^2 \right]. \end{aligned} \tag{24}$$

We show that in the following way. First, let us combine the update steps Equations (8) to (10). Performing change of variable we have:

$$\begin{aligned} w_{ag}^t - w^t &= (1-\alpha_t)w_{ag}^{t-1} + \alpha_t w^{t-1} - \beta_t \nabla l(w_{md}^t) - [w^{t-1} - \lambda_t \nabla l(w_{md}^t)] \\ &= (1-\alpha_t)(w_{ag}^{t-1} - w^{t-1}) + (\lambda_t - \beta_t)\nabla l(w_{md}^t). \end{aligned} \tag{25}$$

Following from Equation (25) and using Lemma 1 stated in (Ghadimi & Lan, 2016) it is implied that:

$$w_{ag}^t - w^t = \Gamma^t \sum_{\tau=1}^{t} \frac{\lambda_\tau - \beta_\tau}{\Gamma^\tau} \nabla l(w_{md}^\tau). \tag{26}$$

Furthermore, we have:

$$||w_{ag}^t - w^t||^2 = \left\| \Gamma^t \sum_{\tau=1}^{t} \frac{\lambda_\tau - \beta_\tau}{\Gamma^\tau} \nabla l(w_{md}^\tau) \right\|^2. \tag{27}$$

From the definition in Equation (13) we have:

$$\sum_{\tau=1}^{t} \frac{\alpha_\tau}{\Gamma^\tau} = \frac{\alpha_1}{\Gamma^1} + \sum_{\tau=2}^{t} \frac{1}{\Gamma^\tau}\left(1 - \frac{\Gamma^\tau}{\Gamma^{\tau-1}}\right) = \frac{1}{\Gamma^1} + \sum_{\tau=2}^{t}\left(\frac{1}{\Gamma^\tau} - \frac{1}{\Gamma^{\tau-1}}\right) = \frac{1}{\Gamma^t}. \tag{28}$$

Inserting that into Equation (27) we get:

$$||w_{ag}^t - w^t||^2 = \left\| \Gamma^t \sum_{\tau=1}^{t} \frac{\alpha_\tau}{\Gamma^\tau} \frac{\lambda_\tau - \beta_\tau}{\alpha^\tau} \nabla l(w_{md}^\tau) \right\|^2. \tag{29}$$

Applying Jensen's inequality to Equation (29) we have:

$$||w_{ag}^t - w^t||^2 \leq \Gamma^t \sum_{\tau=1}^{t} \frac{\alpha_\tau}{\Gamma^\tau} \left\| \frac{\lambda_\tau - \beta_\tau}{\alpha^\tau} \nabla l(w_{md}^\tau) \right\|^2 = \Gamma^t \sum_{\tau=1}^{t} \frac{(\lambda_\tau - \beta_\tau)^2}{\Gamma^\tau \alpha_\tau} ||\nabla l(w_{md}^\tau)||^2. \tag{30}$$

Hence, Equation (24) holds.

Coming back to the main flow of the proof. We combine the previous two inequalities Equation (23) and Equation (24). Also, we use the fact that $\Gamma^{t-1}(1-\alpha_t)^2 \leq \Gamma^t$:

$$\begin{aligned} l(w^t) \leq & l(w^{t-1}) - \lambda_t (1 - \beta\lambda_t) ||\nabla l(w_{md}^t)||^2 + \frac{\beta\lambda_t^2}{2}||\delta^t||^2 - \lambda_t \langle \nabla l(w^{t-1}) - \beta\lambda_t \nabla l(w_{md}^t), \delta^t \rangle \\ & + \frac{\beta\Gamma^t}{2} \sum_{\tau=1}^{t} \frac{(\lambda_\tau - \beta_\tau)^2}{\Gamma^\tau \alpha_\tau} \left[||\nabla l(w_{md}^\tau)||^2 + 2\langle \nabla l(w_{md}^\tau), \delta^\tau \rangle + ||\delta^\tau||^2 \right]. \end{aligned} \tag{31}$$

Summing up the above inequalities (Equation (31)) up to the rTX iterate, we get:

$$\begin{aligned} l(w^{rTX}) &\leq l(w^0) - \sum_{t=1}^{rTX} \lambda_t (1 - \beta\lambda_t) ||\nabla l(w_{md}^t)||^2 - \sum_{t=1}^{rTX} \lambda_t \langle \nabla l(w^{t-1}) - \beta\lambda_t \nabla l(w_{md}^t), \delta^t \rangle \\ &\quad + \sum_{t=1}^{rTX} \frac{\beta\lambda_t^2}{2}||\delta^t||^2 - \frac{\beta}{2} \sum_{t=1}^{rTX} \Gamma^t \sum_{\tau=1}^{t} \frac{(\lambda_\tau - \beta_\tau)^2}{\Gamma^\tau \alpha_\tau} \left[||\nabla l(w_{md}^\tau)||^2 + 2\langle \nabla l(w_{md}^\tau), \delta^\tau \rangle + ||\delta^\tau||^2 \right] \\ &= l(w^0) - \sum_{t=1}^{rTX} \lambda_t C^t ||\nabla l(w_{md}^t)||^2 + \frac{\beta}{2} \sum_{t=1}^{rTX} \lambda_t^2 \left(1 + \frac{(\lambda_t - \beta_t)^2}{\alpha_t \Gamma^t \lambda_t^2} \sum_{\tau=t}^{rTX} \Gamma^\tau \right) ||\delta^t||^2 - \sum_{t=1}^{rTX} b_t, \end{aligned} \tag{32}$$

where $b_t = \langle \lambda_t \nabla l(w^{t-1}) - \left[\beta\lambda_t^2 + \frac{\beta(\lambda_t-\beta_t)^2}{\Gamma^t\alpha_t}\left(\sum_{\tau=t}^{rTX}\Gamma^\tau\right)\right]\nabla l(w_{md}^t), \delta^t\rangle$. Due to the fact that under assumptions Equations (11) and (12) $\mathbb{E}||\delta^t||^2 \leq \sigma^2$ and $\{b_t\}$ is a martingale difference, when taking expectation on both sides we obtain:

$$\sum_{t=1}^{rTX}\lambda_t C^t \mathbb{E}||\nabla l(w_{md}^t)||^2 \leq l(w^0) - l(w^{rTX}) + \frac{\beta\sigma^2}{2}\sum_{t=1}^{rTX}\lambda_t^2\left(1 + \frac{(\lambda_t-\beta_t)^2}{\alpha_t\Gamma^t\lambda_t^2}\sum_{\tau=t}^{rTX}\Gamma^\tau\right). \tag{33}$$

Using the fact that $l(w^t) \geq l(w^*)$, $\mathbb{E}||\nabla l(w_{md}^R)||^2 = \frac{\sum_{t=1}^{rTX}\lambda_t C^t \mathbb{E}||\nabla l(w_{md}^t)||^2}{\sum_{t=1}^{rTX}\lambda_t C^t}$, and by dividing both sides by $\sum_{t=1}^{rTX}\lambda_t C^t$, we obtain:

$$\mathbb{E}||\nabla l(w_{md}^R)||^2 \leq \frac{1}{\sum_{t=1}^{rTX}\lambda_t C^t}\left[l(w^0) - l(w^*) + \frac{\beta\sigma^2}{2}\sum_{t=1}^{T}\lambda_t^2\left(1 + \frac{(\lambda_t-\beta_t)^2}{\alpha_t\Gamma^t\lambda_t^2}\sum_{\tau=t}^{rTX}\Gamma^\tau\right)\right]. \tag{34}$$

Hence, we have proven the wanted Equation (16) holds.

For the remainder of the proof for the nonconvex case we specialize the previously obtained result. Let us assume the following:

$$\alpha_t = \frac{2}{t+1} \tag{35}$$

$$\lambda_t \in \left[\beta_t, \left(1 + \frac{\alpha_t}{4}\right)\beta_t\right] \tag{36}$$

$$\Gamma^t = \frac{2}{t(t+1)} \tag{37}$$

$$\beta_t = \min\left\{\frac{8}{21\beta}, \frac{\tilde{D}}{\sigma\sqrt{rTX}}\right\} \text{ for some } \tilde{D} > 0. \tag{38}$$

Now, we want to prove:

$$\mathbb{E}||\nabla l(w_{md}^R)||^2 \leq \frac{21\beta(l(w^0) - l(w^*))}{4rTX} + \frac{2\sigma}{\sqrt{rTX}}\left(\frac{l(w^0) - l(w^*)}{\tilde{D}} + \beta\tilde{D}\right). \tag{39}$$

From definition of Equation (35), Equation (36) let us make a claim about C^t. For that, from Equation (36) we observe $0 \leq \lambda_t - \beta_t \leq \alpha_t\beta_t/4$. Now we have:

$$C^t = 1 - \beta\left[\lambda_t + \frac{(\lambda_t-\beta_t)^2}{2\alpha_t\Gamma^t\lambda_t}\left(\sum_{\tau=t}^{rTX}\Gamma^\tau\right)\right] \tag{40}$$

$$\geq 1 - \beta\left[\left(1 + \frac{\alpha_t}{4}\right)\beta_t + \frac{\alpha_t^2\beta_t^2}{16}\frac{1}{t\alpha_t\Gamma^t\beta_t}\right] \tag{41}$$

$$= 1 - \beta_t\beta(1 + \frac{\alpha_t}{4} + \frac{1}{16}) \tag{42}$$

$$\geq 1 - \beta_t\beta\frac{21}{16}. \tag{43}$$

Multiplied by λ_t we have $\lambda_t C^t \geq \frac{11\beta_t}{32}$.

Now we make the following claim about Γ^t. From Equation (37):

$$\sum_{\tau=t}^{rTX}\Gamma^\tau = \sum_{\tau=t}^{rTX}\frac{2}{\tau(\tau+1)} = 2\sum_{\tau=t}^{rTX}\left(\frac{1}{\tau} - \frac{1}{\tau+1}\right) \leq \frac{2}{t}. \tag{44}$$

From the Equation (36), Equation (38), Equation (43), we have:

$$C^t \geq 1 - \frac{21}{16}\beta\beta_t \geq \frac{1}{2} > 0 \quad \text{and} \quad \lambda_t C^t \geq \frac{\beta_t}{2}. \tag{45}$$

Furthermore, from Equation (36), Equation (37), Equation (38), and Equation (44), we obtain:

$$\begin{aligned}\lambda_t^2\left[1 + \frac{(\lambda_t - \beta_t)^2}{\alpha_t \Gamma^t \lambda_t^2}\left(\sum_{\tau=t}^{rTX}\Gamma^\tau\right)\right] &\leq \lambda_t^2\left[1 + \frac{1}{\alpha_t\Gamma^t\lambda_t^2}\left(\frac{\alpha_t\beta_t}{4}\right)^2\frac{2}{t}\right] = \lambda_t^2 + \frac{\beta_t^2}{8} \\ &\leq \left[\left(1 + \frac{\alpha_t}{4}\right)^2 + \frac{1}{8}\right]\beta_t^2 \leq 2\beta_t^2.\end{aligned} \tag{46}$$

Together with Equation (34) it holds that:

$$\begin{aligned}\mathbb{E}||\nabla l(w_{md}^R)||^2 &\leq \frac{2}{\sum_{t=1}^{rTX}\beta_t}\left(l(w^0) - l(w^*) + \beta\sigma^2\sum_{t=1}^{rTX}\beta_t^2\right) \\ &\leq \frac{2(l(w^0) - l(w^*))}{rTX\beta_1} + 2\beta\sigma^2\beta_1 \\ &\leq \frac{2(l(w^0) - l(w^*))}{rTX}\left\{\frac{21\beta}{8} + \frac{\sigma\sqrt{rTX}}{\tilde{D}}\right\} + \frac{2\beta\tilde{D}\sigma}{\sqrt{rTX}},\end{aligned} \tag{47}$$

which implies:

$$\mathbb{E}||\nabla l(w_{md}^R)||^2 \leq \frac{21\beta(l(w^0) - l(w^*))}{4rTX} + \frac{2\sigma}{\sqrt{rTX}}\left(\frac{l(w^0) - l(w^*)}{\tilde{D}} + \beta\tilde{D}\right). \tag{48}$$

Hence, we have shown that Equation (48) holds. Continuing from that, minimizing Equation (48) with respect to $\tilde{D}$, the optimal choice is $\tilde{D} = \sqrt{\frac{l(w_{ag}^0) - l(w^*)}{\beta}}$. Inserting that value for $\tilde{D}$, Equation (48) becomes:

$$\mathbb{E}||\nabla l(w_{md}^R)||^2 \leq \frac{21\beta(l(w^0) - l(w^*))}{4rTX} + \frac{4\sigma\sqrt{\beta(l(w^0) - l(w^*))}}{\sqrt{rTX}}. \tag{49}$$

Until now we have assumed that $\mathbb{E}||g(w, \xi_t) - \nabla l(w)||^2 = \sigma^2$ for the ease of the proof. However, if we assume that the gradient is calculated on a batch of size b, the variance of the stochastic gradient reduces to σ^2/b (see (Wang & Srebro, 2019)). The entire previous results follow with that assumption without loss of generality. Therefore we conclude it holds that:

$$\mathbb{E}||\nabla l(w)||^2 \leq \mathcal{O}\left(\frac{\beta(l(w^0) - l(w^*))}{rTX} + \frac{\sigma\sqrt{\beta(l(w^0) - l(w^*))}}{\sqrt{brTX}}\right). \tag{50}$$

Convex case Now, let us consider the case for convex functions. First, in order to prove Equation (5), we want to show that, assuming:

$$\alpha_t\lambda_t \leq \beta\beta_t^2, \quad \beta_t < \frac{1}{\beta}, \tag{51}$$

$$p_t = \frac{\frac{1}{\Gamma^t}\beta_t(1 - \beta\beta_t)}{\sum_{t=1}^{rTX}\frac{1}{\Gamma^t}\beta_t(1 - \beta\beta_t)}, \tag{52}$$

and

$$\frac{\alpha_1}{\lambda_1\Gamma^1} \geq \frac{\alpha_2}{\lambda_2\Gamma^2} \geq \dots \tag{53}$$

the following holds:

$$\mathbb{E}[l(w_{ag}^R - l(w^*))] \leq \frac{\sum_{t=1}^{rTX}\beta_t(1 - \beta\beta_t)\left[(2\lambda_1)^{-1}||w^0 - w^*||^2 + \beta\sigma^2\sum_{j=1}^{t}\frac{\beta_j^2}{\Gamma^j}\right]}{\sum_{t=1}^{rTX}\frac{\beta_t}{\Gamma^t}(1 - \beta\beta_t)}. \tag{54}$$

Starting from the update rule Equation (8) and using the convexity of $l(\cdot)$ we have:

$$\begin{aligned} l(w_{md}^t) - [(1-\alpha_t)l(w_{ag}^{t-1}) + \alpha_t l(w)] &= \alpha_t \left[l(w_{md}^t) - l(w)\right] + (1-\alpha_t)\left[l(w_{md}^t - l(w_{ag}^{t-1}))\right] \\ &\leq \alpha_t \langle \nabla l(w_{md}^t), w_{md}^t - w\rangle + (1-\alpha_t)\langle \nabla l(w_{md}^t), w_{md}^t - w_{ag}^{t-1}\rangle \\ &= \langle \nabla l(w_{md}^t), \alpha_t(w_{md}^t - w) + (1-\alpha_t)(w_{md}^t - w_{ag}^{t-1})\rangle \\ &= \alpha_t \langle \nabla l(w_{md}^t), w^{t-1} - w\rangle. \end{aligned} \tag{55}$$

Similar to before, we now start with the smoothness Equation (17) and use the update step Equation (10) to obtain:

$$\begin{aligned} l(w_{ag}^t) &\leq l(w_{md}^t) + \langle \nabla l(w_{md}^t), w_{ag}^t - w_{md}^t\rangle + \frac{\beta}{2}||w_{ag}^t - w_{md}^t||^2 \\ &= l(w_{md}^t) - \beta_t ||\nabla l(w_{md}^t)||^2 + \beta_t \langle \nabla l(w_{md}^t), \delta^t\rangle + \frac{\beta\beta_t^2}{2}||\nabla l(w_{md}^t) + \delta^t||^2. \end{aligned} \tag{56}$$

Inserting Equation (55) into the previous inequality, we have:

$$\begin{aligned} l(w_{ag}^t) \leq (1-\alpha_t)l(w_{ag}^{t-1}) + \alpha_t l(w) + \alpha_t \langle \nabla l(w_{md}^t), w^{t-1} - w\rangle \\ - \beta_t ||\nabla l(w_{md}^t)||^2 + \beta_t \langle \nabla l(w_{md}^t), \delta^t\rangle + \frac{\beta\beta_t^2}{2}||\nabla l(w_{md}^t) + \delta^t||. \end{aligned} \tag{57}$$

From Equation (10) we have:

$$\begin{aligned} ||w^{t-1} - w||^2 - 2\lambda_t \langle \nabla l(w_{md}^t) + \delta^t, w^{t-1} - w\rangle \\ + \lambda_t^2 ||\nabla l(w_{md}^t) + \delta^t||^2 = ||w^{t-1} - \lambda_t(\nabla l(w_{md}^t) + \delta^t) - w||^2 = ||w^t - w||^2. \end{aligned} \tag{58}$$

From the previous equation, we have:

$$\alpha_t \langle \nabla l(w_{md}^t) + \delta^t, w^{t-1} - w\rangle = \frac{\alpha_t}{2\lambda_t}\left[||w^{t-1} - w||^2 - ||w^t - w||^2\right] + \frac{\alpha_t\lambda_t}{2}||\nabla l(w_{md}^t) + \delta^t||^2. \tag{59}$$

Combining Equations (57) and (59) and the fact that $||\nabla l(w_{md}^t) + \delta^t||^2 = ||\nabla l(w_{md}^t)||^2 + ||\delta^t||^2 + 2\langle \nabla l(w_{md}^t), \delta^t\rangle$, we get:

$$\begin{aligned} l(w_{ag}^t) \leq (1-\alpha_t)l(w_{ag}^{t-1}) + \alpha_t l(w) + \frac{\alpha_t}{2\lambda_t}\left[||w^{t-1} - w||^2 - ||w^t - w||^2\right] \\ - \beta_t \left(1 - \frac{\beta\beta_t}{2} - \frac{\alpha_t\lambda_t}{2\beta_t}\right)||\nabla l(w_{md}^t)||^2 + \left(\frac{\beta\beta_t^2 + \alpha_t\lambda_t}{2}\right)||\delta^t||^2 \\ + \langle \delta^t, (\beta_t + \beta\beta_t^2 + \alpha_t\lambda_t)\nabla l(w_{md}^t) + \alpha_t(w - w^{t-1})\rangle. \end{aligned} \tag{60}$$

Due to the fact that $\alpha_1 = \Gamma^1 = 1$ and by Equation (53) it holds that:

$$\sum_{t=1}^{rTX} \frac{\alpha_t}{\lambda_t \Gamma^t}\left[||w^{t-1} - w||^2 - ||w^t - w||^2\right] \leq \frac{\alpha_1 ||w^0 - w||^2}{\lambda_1 \Gamma^1} = \frac{||w^0 - w||^2}{\lambda_1}. \tag{61}$$

Using Lemma 1 from (Ghadimi & Lan, 2016), Equation (61) and subtracting $l(w)$ from Equation (60), we obtain:

$$\begin{aligned} \frac{l(w_{ag}^{rTX}) - l(w)}{\Gamma^{rTX}} \leq \frac{||w^0 - w||^2}{2\lambda_1} - \sum_{t=1}^{rTX} \frac{\beta_t}{2\Gamma^t}\left(2 - \beta\beta_t - \frac{\alpha_t\lambda_t}{\beta_t}\right)||\nabla l(w_{md}^t)||^2 \\ + \sum_{t=1}^{rTX}\left(\frac{\beta\beta_t^2 + \alpha_t\lambda_t}{2\Gamma^t}\right)||\delta^t||^2 + \sum_{t=1}^{rTX} b_t', \end{aligned} \tag{62}$$

where $b'_t = \frac{1}{\Gamma^t}\langle \delta^t, (\beta_t + \beta\beta_t^2 + \alpha_t\lambda_t)\nabla l(w_{md}^t) + \alpha_t(w - w^{t-1})\rangle$. Together with Equation (51) the above inequality gives:

$$\frac{l(w_{ag}^{rTX}) - l(w)}{\Gamma^{rTX}} \leq \frac{||w^0 - w||^2}{2\lambda_1} - \sum_{t=1}^{rTX} \frac{\beta_t}{\Gamma^t}(1 - \beta\beta_t)||\nabla l(w_{md}^t)||^2 + \sum_{t=1}^{rTX} \frac{\beta\beta_t^2}{\Gamma^t}||\delta^t||^2 + \sum_{t=1}^{rTX} b'_t. \tag{63}$$

Since $\{b'_t\}$ is a martingale difference, $\mathbb{E}||\delta^t||^2 \leq \sigma^2$ and by taking expectation with respect to $\xi_{[rTX]}$, we have:

$$\frac{1}{\Gamma^{rTX}}\mathbb{E}\left[l(w_{ag}^{rTX}) - l(w)\right] \leq \frac{||w^0 - w||^2}{2\lambda_1} - \sum_{t=1}^{rTX} \frac{\beta_t}{\Gamma^t}(1 - \beta\beta_t)\mathbb{E}||\nabla l(w_{md}^t)||^2 + \sigma^2 \sum_{t=1}^{rTX} \frac{\beta\beta_t^2}{\Gamma^t}. \tag{64}$$

Now, assume $w = w^*$ and since by definition $l(w_{ag}^{rTX}) \geq l(w^*)$, we obtain:

$$\sum_{t=1}^{rTX} \frac{\beta_t}{\Gamma^t}(1 - \beta\beta_t)\mathbb{E}||\nabla l(w_{md}^t)||^2 \leq \frac{||w^0 - w^*||^2}{2\lambda_1} + \sigma^2 \sum_{t=1}^{rTX} \frac{\beta\beta_t^2}{\Gamma^t}, \tag{65}$$

from which, using the definition of w_{md}^R, it follows that

$$\mathbb{E}||\nabla l(w_{md}^R)||^2 \leq \frac{(2\lambda_1)^{-1}||w^0 - w^*||^2 + \beta\sigma^2 \sum_{t=1}^{rTX} \frac{\beta_t^2}{\Gamma^t}}{\sum_{t=1}^{rTX} \frac{\beta_t}{\Gamma^t}(1 - \beta\beta_t)}. \tag{66}$$

Also, using Equation (51) and Equation (64) in Equation (65), for $rTX \geq 1$ we have:

$$\mathbb{E}\left[l(w_{ag}^{rTX} - l(w^*))\right] \leq \Gamma^{rTX}\left(\frac{||w^0 - w||^2}{2\lambda_1} + \sigma^2 \sum_{t=1}^{rTX} \frac{\beta\beta_t^2}{\Gamma^t}\right),$$

which implies that Equation (54) holds:

$$\begin{aligned}\mathbb{E}[l(w_{ag}^R - l(w^*))] &= \sum_{t=1}^{rTX} \frac{\frac{\beta_t}{\Gamma^t}(1 - \beta\beta_t)}{\sum_{t=1}^{rTX} \frac{\beta_t}{\Gamma^t}(1 - \beta\beta_t)}\mathbb{E}[l(w_{ag}^t - l(w^*))] \\ &\leq \frac{\sum_{t=1}^{rTX} \beta_t(1 - \beta\beta_t)\left[(2\lambda_1)^{-1}||w^0 - w||^2 + \beta\sigma^2 \sum_{j=1}^{t} \frac{\beta_j^2}{\Gamma^j}\right]}{\sum_{t=1}^{rTX} \frac{\beta_t}{\Gamma^t}(1 - \beta\beta_t)}.\end{aligned} \tag{67}$$

Now, assuming α_t is set as in Equation (35), p_t is set as in Equation (52),

$$\beta_t = \min\left\{\frac{1}{2\beta}, \left(\frac{\tilde{D}^2}{\beta^2\sigma^2(rTX)^3}\right)^{1/4}\right\}, \tag{68}$$

and

$$\lambda_t = \frac{t\beta\beta_t^2}{2}, \tag{69}$$

we want to show that the following inequality holds:

$$\mathbb{E}[l(w_{ag}^R) - l(w^*)] \leq \frac{48\beta||w^0 - w^*||^2}{r^2T^2X^2} + \frac{12\sigma}{\sqrt{rTX}}\left(\frac{||w^0 - w^*||^2}{\tilde{D}} + \tilde{D}\right), \tag{70}$$

for some $\tilde{D} > 0$. Note, that Equation (68) and Equation (69) imply Equation (53) and Equation (51).

Since, $\Gamma^t = \frac{2}{t(t+1)}$, and by Equation (68), we obtain:

$$\sum_{t=1}^{rTX} \frac{\beta_t}{\Gamma^t}(1-\beta\beta_t) \geq \frac{1}{2}\sum_{t=1}^{rTX}\frac{\beta_t}{\Gamma^t} = \frac{\beta_1}{2}\sum_{t=1}^{rTX}\frac{1}{\Gamma^t} \tag{71}$$

$$\sum_{t=1}^{rTX}\frac{1}{\Gamma^t} \geq \sum_{t=1}^{rTX}\frac{t^2}{2} = \frac{1}{12}rTX(rTX+1)(2rTX+1) \geq \frac{1}{6}r^3T^3X^3. \tag{72}$$

By $\Gamma^t = \frac{2}{t(t+1)}$, Equations (66), (68) and (69), we obtain:

$$\begin{aligned}
\mathbb{E}||\nabla l(w_{md}^R)||^2 &\leq \frac{2}{\beta_1\sum_{t=1}^{rTX}\frac{1}{\Gamma^t}}\left(\frac{||w^0-w^*||^2}{\beta\beta_1^2} + \beta\sigma^2\beta_1^2\sum_{t=1}^{rTX}\frac{1}{\Gamma^t}\right) \\
&= \frac{2||w^0-w^*||^2}{\beta\beta_1^3\sum_{t=1}^{rTX}\frac{1}{\Gamma^t}} + 2\beta\sigma^2\beta_1 \leq \frac{12||w^0-w^*||^2}{\beta r^3T^3X^3\beta_1^3} + 2\beta\sigma^2\beta_1 \\
&\leq \frac{96\beta^2||w^0-w^*||^2}{r^3T^3X^3} + \frac{\beta^{1/2\sigma^{3/2}}}{(rTX)^{3/4}}\left(\frac{12||w^0-w^*||^2}{\tilde{D}^{3/2}} + 2\tilde{D}^{1/2}\right).
\end{aligned} \tag{73}$$

Moreover, by Equation (68), it holds that:

$$1-\beta\beta_t \leq 1 \quad \text{and} \quad \sum_{j=1}^{t}\frac{1}{\Gamma^j} = \frac{1}{2}\sum_{j=1}^{t}j(j+1) \leq \sum_{j=1}^{t}j^2 \leq t^3.$$

It is implied by Equations (67), (68), (71) and (72) that:

$$\begin{aligned}
\mathbb{E}[l(w_{ag}^R) - l(w^*)] &\leq \frac{2}{\sum_{t=1}^{rTX}\frac{1}{\Gamma^t}}\left[rTX(2\lambda_1)^{-1}||w^0-w^*||^2 + \beta\sigma^2\beta_1^2\sum_{t=1}^{rTX}t^3\right] \\
&\leq \frac{12||w^0-w^*||^2}{r^2T^2X^2\beta\beta_1^2} + \frac{12\beta\sigma^2\beta_1^2}{r^3T^3X^3}\sum_{t=1}^{rTX}t^3 \\
&\leq \frac{12||w^0-w^*||^2}{r^2T^2X^2\beta\beta_1^2} + 12\beta\sigma^2\beta_1^2rTX \\
&\leq \frac{48\beta||w^0-w^*||^2}{r^2T^2X^2} + \frac{12\sigma}{\sqrt{rTX}}\left(\frac{||w^0-w^*||^2}{\tilde{D}} + \tilde{D}\right).
\end{aligned} \tag{74}$$

This shows that Equation (70) holds. Minimizing the previous inequality with respect to $\tilde{D}$, the optimal choice is $\tilde{D} = ||w^0 - w^*||$. Hence, it becomes:

$$\mathbb{E}[l(w_{ag}^R) - l(w^*)] \leq \frac{48\beta||w^0-w^*||^2}{r^2T^2X^2} + \frac{24||w^0-w^*||\sigma}{\sqrt{rTX}}. \tag{75}$$

As in (Wang & Srebro, 2019), the variance of the stochastic gradient reduces to σ^2/b when estimating with b samples. Therefore we conclude it holds that:

$$\mathbb{E}[l(w) - l(w^*)] \leq \mathcal{O}\left(\frac{\beta||w^0-w^*||^2}{r^2T^2X^2} + \frac{\sigma||w^0-w^*||}{\sqrt{brTX}}\right). \tag{76}$$

□

F. RS2 Generalization Error

We proceed with the generalization error bound of RS2 for nonconvex Lipschitz and smooth losses. We start by introducing the assumptions on the function $f : \mathbb{R}^d \times \mathcal{Z} \to \mathbb{R}^+$ (see Section 4) for completeness, and then we proceed with the proof of Theorem 4.2.

Assumption. (Smooth and Lipschitz Loss) There exist constants $\beta_f \geq 0$ and $L_f \geq 0$, such that for all $w, u \in \mathbb{R}^d$ and $x \in \mathcal{X}$, it is true that $\|\nabla_w f(w,z) - \nabla_u f(u,z)\|_2 \leq \beta_f \|w-u\|_2$ and $\|f(w,z) - f(u,z)\|_2 \leq L_f \|w-u\|_2$.

The next result follows form prior work (Nikolakakis et al., 2023) and it suffices to show that RS2 sampling is data independent and belongs to the set of general mini batch schedules that appear in Nikolakakis et al. (2023, Definition 1).

Theorem F.1 (Generalization error of standard gradient RS2, (Nikolakakis et al., 2023) Theorem 8)**.** *Let the function f be nonconvex, L_f-Lipschitz and β_f-smooth. Then the generalization error of the standard gradient RS2 algorithm with a decreasing step-size $\eta_t \leq C/t$ (for $C < 1/\beta_f$), is bounded as:*

$$|\epsilon_{\text{gen}}(f, \mathcal{D}, \text{RS2})| \leq \frac{1}{N} \cdot 2Ce^{C\beta_f} L_f^2 (r \cdot T \cdot X)^{C\beta_f} \min\Big\{1 + \frac{1}{C\beta_f}, \log(e \cdot r \cdot T \cdot X)\Big\}. \tag{77}$$

Proof. Let $\{k_1^j, \ldots, k_b^j\} \subset \{1, 2, \ldots, N\}^b$ be the set of indices for mini batch selection at each gradient step $j \in \{1, \ldots, rTX\}$. We select the mini batch through the choice of indices $\{k_1^j, \ldots, k_b^j\}$ as follows. For sampling with replacement in line 4 of Algorithm 1 at round j selects a subset of indices $\{k_1^j, \ldots, k_{rN}^j\}$. These indices are sampled independently from any other round $i \in \{1, \ldots, X\}$, i.e., the same indices can be sampled in consecutive rounds, hence with replacement. Note, that at round j sampled indices in the set are unique. The parameters are then updated using a deterministic batch schedule iterating through the sampled subset of indices resulting in rT gradient updates. On the contrary, RS2 without replacement can be seen as traversing the full dataset in a deterministic round-Robin fashion. That is, the model parameters are updated by sequentially selecting indices $\{k_1^j, \ldots, k_b^j\}$. After iterating over the full dataset, i.e., after $T = N/b$ gradient updates we shuffle the full dataset array and repeat the procedure (e.g., Algorithm 3). The algorithm early stops after rTX gradient updates. Thus the selection rule is non-adaptive and data-independent and it belongs to the set of the general batch schedules Nikolakakis et al. (2023, Definition 1). As a consequence, Nikolakakis et al. (2023, Lemma 2) and the growth recursion Nikolakakis et al. (2023, Lemma 3 (Growth Recursion)) holds verbatim for RS2 with standard gradient training with batch size b. Then, we solve the recursion identically to Nikolakakis et al. (2023, Proof of Theorem 8)) for rTX total number of gradient steps. The solution of the recursion gives (the on-average stability and thus) the generalization error bound of RS2, as appears in the theorem, and completes the proof. □